

---

# The Minimax Rate of Second-Order Calibration

---

Kamil Ciosek  
Spotify

Banafsheh Rafiee  
Spotify

Sina Ghiassian  
Spotify

Nicolò Felicioni  
Spotify

## Abstract

We characterize the minimax rate of estimating the second-order calibration error for binary classification, which quantifies whether a higher-order predictor’s epistemic-uncertainty estimate matches the conditional variance of the label probability on its level sets. Our key observation is that the sech perturbation kernel, previously used only to enforce smoothness of calibration functions, in fact makes them *analytic* in a strip of half-width  $h\pi/2$ . Polynomial regression then estimates the calibration error at rate  $\tilde{O}(1/\sqrt{n})$ , with explicit constants, a qualitative improvement over the  $O(n^{-1/4})$  rate achievable by bucketing or kernel smoothing. A matching  $\Omega(1/\sqrt{n})$  lower bound establishes minimax optimality up to logarithmic factors. As a corollary, we give the first finite-sample guarantee for second-order Platt scaling, yielding a post-hoc procedure that recalibrates both the mean prediction and the epistemic-variance estimate of any higher-order predictor. Along the way, we provide a bucket-free definition of second-order calibration and relate it quantitatively to the bucketed formulation of Ahdriz et al. [2025]. Our experiments confirm the predicted rate and the quality of the recalibrated uncertainties.

## 1 Introduction

Modern predictors often output not just a probability but also an uncertainty estimate. A deep ensemble, a Bayesian neural network, or an evidential model produces, for an input  $x$ , a mean prediction  $m(x)$  together with a disagreement measure  $\sigma^2(x)$  intended to capture epistemic uncertainty. Whether  $\sigma^2$  actually has this meaning is a separate question from how it was produced. Ahdriz et al. [2025] gave a precise characterisation:  $\sigma^2$  captures epistemic uncertainty exactly when the predictor is *higher-order calibrated*. A calibrated  $\sigma^2$  separates inherent ambiguity (aleatoric uncertainty) from resolvable ignorance (epistemic uncertainty). We propose to measure such second-order calibration (and thus the quality of epistemic uncertainty) using the second-order calibration error, in analogy to the well-known first-order calibration error [Błasiok et al., 2023, Lee et al., 2023].

This raises two basic statistical questions. How many 2-snapshots are needed to *estimate* the second-order calibration error of a given predictor, and at what rate? And how can one *correct* a miscalibrated  $(m, \sigma^2)$  so that its epistemic uncertainty acquires real-world semantics, with finite-sample guarantees? Ahdriz et al. [2025] addressed both through a bucketing of the score space, but provided no finite-sample bounds; the natural distribution-free alternatives ie. bucketing or kernel-smoothing the two-dimensional score  $(m, \sigma^2)$  give only nonparametric  $n^{-1/4}$  rates, which leave  $\widehat{\text{CE}}_2$  indistinguishable from a constant at moderate sample sizes.

We show that this rate is far from optimal. The key observation is that the sech perturbation kernel of Ciosek et al. [2026], used in the first-order setting only to enforce smoothness, in fact makes the perturbed calibration functions *analytic in a complex strip of half-width  $h\pi/2$* . Via the Bernstein-ellipse theorem, polynomial regression then estimates  $\text{CE}_2$  at rate  $\tilde{O}(1/\sqrt{n})$  with explicit constants. This is a qualitative improvement over  $n^{-1/4}$  and matches  $\Omega(1/\sqrt{n})$  Le Cam lower bound, proving minimax-optimality up to logarithmic factors. As a corollary, the same construction yields the first

post-hoc recalibration procedure for  $(m, \sigma^2)$  with a finite-sample second-order calibration guarantee, which we call second-order Platt scaling.

**Contributions.** We make the following contributions.

1. **Definitions Without Bucketing:** we provide definitions of second-order calibration without relying on any bucketing scheme.
2. **Analyticity** (lemma 1): the sech-perturbed calibration function is analytic in a strip of half-width  $h\pi/2$ . This is the core theoretical observation that enables everything else.
3. **Estimation at  $\tilde{O}(1/\sqrt{n})$**  (proposition 1): polynomial regression exploits analyticity to estimate  $\text{CE}_2$  at rate  $O(\log^{3/2} n/\sqrt{n})$  from 2-snapshots. This is the first finite-sample bound for second-order calibration error and dramatically improves over the  $O(n^{-1/4})$  rate obtainable with kernel smoothing or bucketing.
4. **Rate Tightness** We provide (proposition 2) a  $\Omega(1/\sqrt{n})$  lower bound on the rate, matching the upper bound up to log factors. This provides a complete data efficiency characterization of second-order calibration.
5. **Second-order Platt scaling** (proposition 3): remapping through the estimated calibration functions yields a predictor that is approximately second-order calibrated at the same  $\tilde{O}(1/\sqrt{n})$  rate.

## 2 Setup

We study binary classification with  $Y \in \{0, 1\}$ . Nature generates i.i.d. data;  $f^*(x) = P(Y=1 | X=x)$ . We make no assumptions on  $f^*$  or the marginal of  $X$  i.e. we are in the distribution-free setting. We have  $n$  i.i.d. 2-snapshots  $(X_i, Y_i^{(1)}, Y_i^{(2)})$  with  $Y_i^{(1)}, Y_i^{(2)} | X_i \stackrel{\text{i.i.d.}}{\sim} \text{Bernoulli}(f^*(X_i))$ .

**Definition 1** (Higher-order predictor and calibration). *A higher-order predictor maps  $x \mapsto S(x) = (m(x), \sigma^2(x))$  with  $m \in [0, 1]$ ,  $\sigma^2 \in [0, m(1-m)]$ . Its calibration functions are*

$$\eta_1(s) = \mathbb{E}[Y | S(X) = s], \quad \eta_2(s) = \mathbb{E}[f^*(X)^2 | S(X) = s], \quad (1)$$

and the second-order calibration error is

$$\text{CE}_2 = \mathbb{E}[|\eta_1(S) - m|] + \mathbb{E}[|\eta_2(S) - v|] \quad (2)$$

with  $v = m^2 + \sigma^2$ .

**Intuitions.** We will now provide intuitions about the usefulness of definition 1. The law of total variance can always be used to write

$$\underbrace{\eta_1(s)(1 - \eta_1(s))}_{\text{total}} = \underbrace{\mathbb{E}[f^*(X)(1-f^*(X)) | S=s]}_{\text{aleatoric}} + \underbrace{\text{Var}(f^*(X) | S=s)}_{\text{epistemic}}. \quad (3)$$

When  $\text{CE}_2 = 0$  i.e. for a second order calibrated classifier, we can further write

$$\text{Var}(f^*(X) | S=s) = \underbrace{\mathbb{E}[(f^*(X))^2 | S=s]}_{\eta_2(s)=v} - \underbrace{\mathbb{E}[f^*(X) | S=s]^2}_{\eta_1(s)=m} = v - m^2 = \sigma^2$$

This means that calibration allows us to interpret  $\sigma^2$  as a measure of epistemic uncertainty. A high-level comparison between first and second-order calibration is given in table 1. Note that while the definition of second-order calibration given here is ostensibly different from the definition due to Ahdritz et al. [2025], the two versions are in fact very closely related (see appendix D for a discussion). See figure 1 for further illustrations of calibration functions and how they relate to epistemic vs aleatoric uncertainty.<sup>1</sup>

**Goals.** The main computational goals of this work are to estimate the quantity (2) using as little data as possible; moreover we study the usefulness of calibration functions in (1) to calibrate second-order uncertainty, in a way analogous to Platt scaling.

<sup>1</sup>The observation that ambiguity is connected to epistemic uncertainty has been made by Osband et al. [2023] in the context of epistemic neural networks, a specific way of obtaining uncertainty estimates.

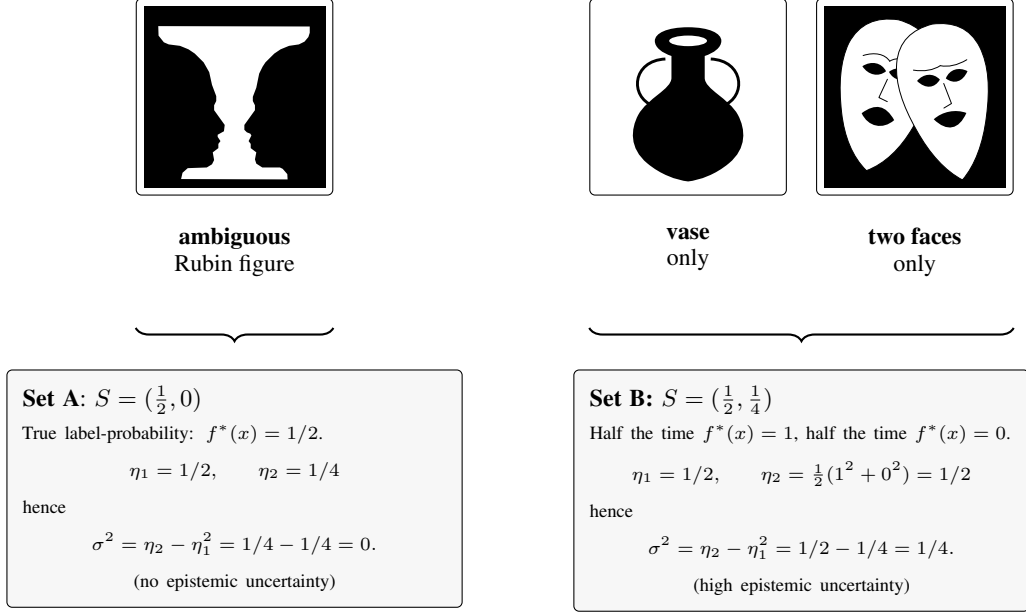


Figure 1: Why second-order calibration is useful. Both sets have the same mean prediction  $m = 1/2$ , so a first-order calibrated predictor treats them identically. But Set A’s Rubin figures are genuinely 50:50 (aleatoric,  $\sigma^2 = 0$ ), while Set B mixes clear vases with clear faces that the classifier hasn’t seen enough data to tell apart (epistemic,  $\sigma^2 = 1/4$ ). A calibrated  $\sigma^2$  distinguishes inherent ambiguity from resolvable ignorance.

|           | First-order                            | Second-order (this paper)                           |
|-----------|--|---|
| Output    | probability $s$                        | $(m, \sigma^2)$                                     |
| Data      | labels $Y_i$                           | 2-snapshots $(Y_i^{(1)}, Y_i^{(2)})$                |
| Measure   | $\eta(s) = \mathbb{E}[Y   S=s]$        | $\eta_1(s), \eta_2(s)$                              |
| Diagnose  | $\text{CE}_1 = \mathbb{E}[ \eta - s ]$ | $\text{CE}_2$                                       |
| Fix       | $s \mapsto \eta(s)$                    | $(m, \sigma^2) \mapsto (\eta_1, \eta_2 - \eta_1^2)$ |
| Guarantee | calibrated probabilities               | calibrated epistemic uncertainty                    |
| Rate      | $\tilde{O}(1/\sqrt{n})$                | $\tilde{O}(1/\sqrt{n})$                             |

Table 1: Comparison of first and second order calibration.

### 3 The Sech Perturbation, Analyticity and Estimation

**Key insight: analyticity.** In order to achieve sample efficiency on the order of  $\tilde{O}(1/\sqrt{n})$ , we leverage the sech perturbation kernel technique, used by Ciosek et al. [2026] to enforce smoothness of calibration first-order calibration functions. Crucially, we observe that the sech perturbation produces calibration functions that are not merely twice differentiable but *analytic*. Specifically, analytic in a strip of width  $h\pi/2$  around the real axis, where  $h$  is the perturbation bandwidth. We will see that, by the classical Bernstein ellipse theorem, analytic functions are approximated by polynomials at an exponential rate. This converts the estimation problem from nonparametric regression (with polynomial rates like  $n^{-1/4}$ ) to essentially parametric regression in a slowly growing polynomial basis (with near- $1/\sqrt{n}$  rates).

#### 3.1 The perturbation scheme

Similarly to Ciosek et al. [2026], we perturb the predictor’s scores by adding noise from a sech kernel. This is a design choice: the perturbed predictor is the one we deploy and recalibrate.

**Definition 2** (Sech perturbation). For a score  $s \in [a, b]$  and bandwidth  $h > 0$ , the perturbation kernel is

$$k_h(t | s) = \frac{\operatorname{sech}\left(\frac{t-s}{h}\right)}{Z(s, h)} \cdot \mathbf{1}_{[a, b]}(t), \quad Z(s, h) = \int_a^b \operatorname{sech}\left(\frac{u-s}{h}\right) du. \quad (4)$$

The perturbed score  $S \sim k_h(\cdot | s)$  satisfies  $S \in [a, b]$ .

Since we have a 2D score space, we will use a *product perturbation* on the rectangle  $\mathcal{R} = [0, 1] \times [0, \frac{1}{4}]$  i.e. draw each coordinate independently:

**Step 1.** Draw  $m \sim k_h(\cdot | m_{\text{orig}})$  on  $[0, 1]$ .

**Step 2.** Draw  $\sigma^2 \sim k_h(\cdot | \sigma_{\text{orig}}^2)$  on  $[0, \frac{1}{4}]$ , independently.

The rectangle  $\mathcal{R}$  contains the feasible region  $\mathcal{F} = \{(m_{\text{orig}}, \sigma_{\text{orig}}^2) : \sigma_{\text{orig}}^2 \leq m_{\text{orig}}(1 - m_{\text{orig}})\}$ , so all original scores lie inside  $\mathcal{R}$ . The perturbed score  $(m, \sigma^2)$  may fall outside  $\mathcal{F}$  but always lies in  $\mathcal{R}$ . While definition 1 works for any binary classifier, the estimation process we describe is designed for classifiers *perturbed* using the process described in this section. Crucially, this makes the calibration functions analytic, which enables quick estimation. While this perturbation ostensibly looks like a major constraint, Ciosek et al. [2026] show that perturbation on the order of  $h = 2^{-6}$  does not degrade classifier performance in practice. They also argue that estimating calibration order is impossible without either the perturbation or other structural assumptions on the calibration functions, even in the first-order case. Hence all our practical results concern the perturbed classifier. We use

### 3.2 The analyticity lemma

The following lemma (proved in appendix C.2 is the centerpiece of our analysis: we show that calibration functions of the perturbed classifier are analytic, which later enables their extremely data-efficient approximation with polynomials.

**Lemma 1** (Analyticity of perturbed calibration functions). *Let  $S$  be any higher-order predictor with calibration functions  $\eta_1^{\text{orig}}, \eta_2^{\text{orig}}$ . Let  $\eta_1, \eta_2$  be the calibration functions of the sech-perturbed predictor with bandwidth  $h > 0$  (using product perturbation in 2D).*

**(1D)** *If  $S(x) = m(x) \in [0, 1]$  is a scalar score, then  $\eta_1$  is analytic in the strip  $\{z \in \mathbb{C} : |\operatorname{Im}(z)| < h\pi/2\} \cap \{z \in \mathbb{C} : 0 \leq \operatorname{Re}(z) \leq 1\}$ .*

**(2D)** *For the full score  $S(x) = (m(x), \sigma^2(x))$  with product perturbation,  $\eta_j$  ( $j = 1, 2$ ) is analytic in  $m$  in the strip  $|\operatorname{Im}(m)| < h\pi/2$  for each fixed real  $\sigma^2$ , and analytic in  $\sigma^2$  in the strip  $|\operatorname{Im}(\sigma^2)| < h\pi/2$  for each fixed real  $m$ .*

### 3.3 Polynomial Estimation

We state a classical result (proved in appendix C.3 in our notation) on function approximation with polynomials, in a form adapted to our setting.

**Lemma 2** (Bernstein ellipse theorem on  $[0, 1]$ ). *Let  $f : [0, 1] \rightarrow \mathbb{R}$  be the restriction of a function analytic in the strip  $|\operatorname{Im}(z)| < \rho$  around  $[0, 1]$ , with  $\sup_{|\operatorname{Im}(z)| < \rho} |f(z)| \leq M$ . Then for every integer  $l \geq 0$ , there exists a polynomial  $q_l$  of degree  $l$  with*

$$\sup_{t \in [0, 1]} |f(t) - q_l(t)| \leq 2M \frac{\theta^{-l}}{\theta - 1},$$

where  $\theta = 2\rho + \sqrt{4\rho^2 + 1} > 1$  is the Bernstein ellipse parameter.

**Corollary 1** (Polynomial approximation of  $\eta$ ). *The perturbed calibration functions  $\eta_1, \eta_2$  on  $[0, 1]$  (1D) or on  $\mathcal{R}$  (2D) are approximated by degree- $l$  (tensor product) polynomials at rate  $\varepsilon_l \leq B_\theta \theta^{-l} = O(\theta^{-l})$  (where  $B_\theta = \frac{2}{\theta-1}$ ) in sup norm, where  $\theta = h\pi + \sqrt{h^2\pi^2 + 1} > 1$  (with the strip half-width  $\rho = h\pi/2$  from Lemma 1). Here, we set  $M = 1$  conservatively.*

For fixed bandwidth  $h$ , the parameter  $\theta > 1$  is a constant. Choosing  $l = \lceil 2 \log n / \log \theta \rceil$  makes  $\varepsilon_l = O(n^{-2})$ , negligible compared to the estimation error.

### 3.4 The estimator

Let  $\mathcal{P}_l$  denote the class of functions on  $\mathcal{R}$  of the form  $f(m, \sigma^2) = \text{clip}_{[0,1]}(\beta^\top \phi(m, \sigma^2))$ , where  $\phi$  is the tensor product polynomial basis of degree  $l$  in each variable (so  $\phi$  has  $d = (l + 1)^2$  components), and  $\text{clip}_{[0,1]}$  projects to  $[0, 1]$ .

Given 2-snapshots  $(X_i, Y_i^{(1)}, Y_i^{(2)})_{i=1}^n$  with perturbed scores  $S_i = (m_i, \sigma_i^2)$  and products  $P_i = Y_i^{(1)} Y_i^{(2)}$ :

$$\hat{\eta}_1 = \arg \min_{f \in \mathcal{P}_l} \frac{1}{n} \sum_{i=1}^n (Y_i^{(1)} - f(S_i))^2, \quad (5)$$

$$\hat{\eta}_2 = \arg \min_{f \in \mathcal{P}_l} \frac{1}{n} \sum_{i=1}^n (P_i - f(S_i))^2. \quad (6)$$

Both are empirical risk minimization (ERM) over the same function class  $\mathcal{P}_l$ , with different response variables ( $Y_i^{(1)} \in \{0, 1\}$  for  $\hat{\eta}_1$ ;  $P_i \in \{0, 1\}$  for  $\hat{\eta}_2$ ).

The CE estimator is:

$$\widehat{\text{CE}}_2 = \frac{1}{n} \sum_{i=1}^n |\hat{\eta}_1(S_i) - \tilde{m}_i| + \frac{1}{n} \sum_{i=1}^n |\hat{\eta}_2(S_i) - (\tilde{m}_i^2 + \tilde{\sigma}_i^2)|. \quad (7)$$

## 4 Main Result

We now show our main result (proved in appendix C.6), which characterizes the rate of convergence of the estimator to the ground truth.

**Proposition 1** (Estimation of  $\text{CE}_2$  at near-parametric rate). *Fix the perturbation bandwidth  $h > 0$  and let  $\theta = h\pi + \sqrt{h^2\pi^2 + 1}$ . Set the polynomial degree to  $l = \lceil 2 \log n / \log \theta \rceil$ , so that  $d = (l + 1)^2 = O(\log^2 n)$ . Then the estimator (7) satisfies*

$$\mathbb{E}[|\widehat{\text{CE}}_2 - \text{CE}_2^{\text{pert}}|] = O\left(\frac{\log^{3/2} n}{\sqrt{n}}\right), \quad (8)$$

where  $\text{CE}_2^{\text{pert}}$  is the second-order calibration error of the perturbed predictor. The constant depends on  $h$  (through  $\theta$ ) and on the sech kernel, but not on the score distribution or the original calibration functions.

Moreover, we can use essentially the same technique to obtain a novel result about first-order calibration; this is reflected in the remark below.

**Remark 1** (First-Order Calibration). *While proposition 1 does not immediately relate to first-order calibration<sup>2</sup>, estimating the first-order calibration error  $\text{CE}_1 = \mathbb{E}[|\mathbb{E}[Y | m] - m|]$  can be accomplished in a straightforward way using the same technique, yielding the same near- $1/\sqrt{n}$  rate.*

**Rate comparison.** The table below compares the rates obtainable with various approaches. It can be seen that our method comes with the best rate.

| Method                                       | Rate for $\text{CE}_2$ estimation              |
|--|--|
| Bucketing Ahdriz et al. [2025]               | no certified rate                              |
| Bucketing + perturbation                     | $O(n^{-1/4})$                                  |
| Kernel regression + perturbation             | $O(n^{-1/4})$                                  |
| <b>Polynomial + analyticity (this paper)</b> | <b><math>O(\log^{3/2} n / \sqrt{n})</math></b> |

<sup>2</sup>In first-order calibration, the conditioning is only wrt. the mean, ignoring the epistemic variance.

## 5 Lower Bound on Rate and Minimax Optimality

To complement our results about the rate, we also provide the following lower bound result (proven in appendix E), which establishes that our rate is optimal (up to log factors). Propositions 1 and 2, taken together, provide a complete characterization of the sample complexity of second-order calibration.

**Proposition 2** (Minimax lower-bound on rate). *There exists an absolute constant  $c > 0$  such that, for every sech bandwidth  $h > 0$ , every  $n \geq 1$ , and every estimator  $\widehat{\text{CE}}_2$ , two distributions  $P_0, P_1$  in the setup of the main paper exist with*

$$\max_{b \in \{0,1\}} \mathbb{E}_{P_b} [ |\widehat{\text{CE}}_2 - \text{CE}_2^{\text{pert}}(P_b)| ] \geq \frac{c}{\sqrt{n}}.$$

The constant  $c$  does not depend on  $h$ .

## 6 Second-Order Platt Scaling

### 6.1 The recalibration map

Given calibration functions  $\eta_1, \eta_2$  (true or estimated), define the *recalibrated predictor*:

$$T(x) = \left( \underbrace{\eta_1(S(x))}_{m'(x)}, \underbrace{\eta_2(S(x)) - \eta_1(S(x))^2}_{(\sigma^2)'(x)} \right), \quad (9)$$

where  $S(x)$  is the perturbed score.

**Proposition 3** (Exact second-order Platt scaling). *If  $\eta_1, \eta_2$  are the true calibration functions, then  $T$  is perfectly second-order calibrated with respect to its own level sets:*

$$\mathbb{E}[Y \mid T(X) = (m', (\sigma^2)')] = m', \quad (10)$$

$$\mathbb{E}[f^*(X)^2 \mid T(X) = (m', (\sigma^2)')] = (m')^2 + (\sigma^2)'. \quad (11)$$

*Proof.* **First moment.** By the tower property:

$$\mathbb{E}[Y \mid T(X) = (m', (\sigma^2)')] = \mathbb{E} \left[ \underbrace{\mathbb{E}[Y \mid S(X)]}_{=\eta_1(S(X))=m'(X)} \mid T(X) = (m', (\sigma^2)') \right].$$

On the event  $\{T(X) = (m', (\sigma^2)')\}$ , the first component  $m'(X) = m'$  is constant. So the expression equals  $m'$ .

**Second moment.** Similarly:

$$\mathbb{E}[f^*(X)^2 \mid T(X) = (m', (\sigma^2)')] = \mathbb{E}[\eta_2(S(X)) \mid T(X) = (m', (\sigma^2)')].$$

Now  $\eta_2(S(X)) = \eta_1(S(X))^2 + (\eta_2(S(X)) - \eta_1(S(X))^2) = m'(X)^2 + (\sigma^2)'(X)$ . On the conditioning event, this equals  $(m')^2 + (\sigma^2)'$ .  $\square$

### 6.2 Approximate guarantee from finite data

We now want to show that the second-order Platt scaling “works” in the sense that the re-calibrated predictor is well-calibrated. In practice, in order to perform the re-calibration, we use the estimated  $\hat{\eta}_1, \hat{\eta}_2$  from Section 3.3:

$$\hat{T}(x) = (\hat{\eta}_1(S(x)), \max(0, \hat{\eta}_2(S(x)) - \hat{\eta}_1(S(x))^2)). \quad (12)$$

The clipping at zero handles estimation noise. Persistent negativity at a score  $s$  indicates the model overestimates its epistemic uncertainty at  $s$ .

**Corollary 2.** *Under the assumptions of Proposition 1, the recalibrated predictor  $\hat{T}$  satisfies  $\mathbb{E}[\text{CE}_2(\hat{T})] = O(\log^{3/2} n / \sqrt{n})$ .*

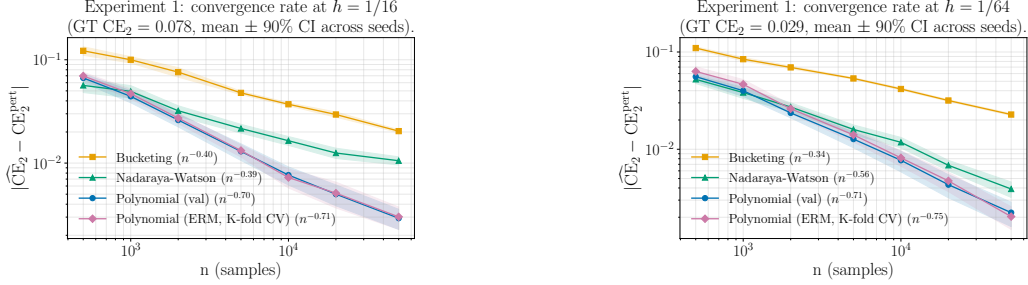


Figure 2: **Experiment 1 (rate)**.  $|\widehat{\text{CE}}_2 - \text{CE}_2^{\text{pert}}|$  vs.  $n$  at  $h=1/16$  (left) and  $h=1/64$  (right); mean  $\pm$  Student- $t$  90% CI across 20 seeds, log-log slopes in legend.

*Proof sketch.* The first-moment calibration error of  $\hat{T}$  is  $\mathbb{E}[|\mathbb{E}[Y | \hat{T}] - m'(X)|]$ . By the tower property,  $\mathbb{E}[Y | \hat{T}] = \mathbb{E}[\eta_1(S) | \hat{T}]$ . Since  $m'(X) = \hat{\eta}_1(S(X))$ :

$$\mathbb{E}[|\mathbb{E}[\eta_1 | \hat{T}] - \hat{\eta}_1|] \leq \mathbb{E}[|\eta_1(S) - \hat{\eta}_1(S)|] = \|\eta_1 - \hat{\eta}_1\|_{L^1(P)} = O\left(\frac{\log^{3/2} n}{\sqrt{n}}\right),$$

where the inequality is Jensen’s (conditional expectation contracts  $L^1$  distance). The second-moment bound is analogous.  $\square$

## 7 Experiments

Our four experiments mirror the chain of theoretical claims. Experiment 1 verifies the predicted near- $1/\sqrt{n}$  rate of Proposition 1; Experiment 2 confirms that the resulting recalibrator  $\hat{T}$  delivers the calibrated  $(\sigma^2)'$  promised by Corollary 2; Experiment 3 isolates *why* that calibration is worth doing — its *magnitude*, not just its ranking, controls downstream decisions; and Experiment 4 reproduces the same effect on real labels. Experiments 1–3 use synthetic data with known ground truth, Experiment 4 uses the public Weather Sentiment AMT dataset.

**Experiment 1 — the predicted rate.** The DGP is a 10-component Gaussian mixture in  $\mathbb{R}^4$  with  $f^*(x) = \sigma(w^\top x)$ ; the predictor is a 5-member MLP ensemble whose mean and unbiased variance are sech-perturbed coordinate-wise. Ground-truth  $\text{CE}_2^{\text{pert}}$  is computed by quasi-Monte Carlo (replicate spread  $< 2 \cdot 10^{-5}$ ). We compare 2D bucketing, Nadaraya–Watson with an isotropic Gaussian kernel, and our polynomial estimator (held-out and CV-tuned variants); baseline bin counts and bandwidths follow textbook MISE rules with constants tuned on a held-out split. Figure 2 shows that the polynomial estimator dominates at every  $n$ , with empirical log–log slope  $\approx -0.70$  at both  $h \in \{1/16, 1/64\}$  — at least as steep as the predicted  $-1/2$  rate and steeper than the  $-0.33$  to  $-0.55$  slopes of bucketing and NW (consistent with their distribution-free Lipschitz rate). The two polynomial variants are indistinguishable, so the advantage is not an artefact of held-out tuning. Setup details in App. B.1.

**Experiment 2 — the recalibrated  $\sigma^2$  tracks the truth.** We replace the predictor with a 20-member ensemble deliberately undertrained so that its raw  $\sigma^2$  carries only a faint epistemic signal; the recalibrator is a tensor-Chebyshev ridge regression of degree 12 fit on  $2 \cdot 10^4$  2-snapshots. Ground-truth conditional variance at perturbed scores is obtained by sech-smoothing the empirical  $(p, p^2)$  joint of the DGP. The raw  $\sigma^2$  is essentially uncorrelated with truth (Pearson 0.10), but after applying  $\hat{T}$  the scatter concentrates on the diagonal (Pearson 0.74); see Figure 3. Across 20 calibration seeds,  $\text{CE}_2$  drops from 0.37 to  $0.04 \pm 0.01$  — exactly the rate-driven recalibration guarantee of Corollary 2 cashing out empirically. App. B.2.

**Experiment 3 — magnitudes, not just rankings.** A clinic refers borderline patients ( $m \in [0.35, 0.65]$ ) at cost  $c=0.06$  for a noisy specialist panel; the per-patient gain  $g(\theta) = 2\theta^2 - 2\theta + 0.5 - c$  has conditional mean  $2\eta_2(S) - 2\eta_1(S) + 0.5 - c$ , so any post-hoc procedure that calibrates only  $\eta_1$  is misspecified for the Bayes-optimal score. The borderline cohort splits into an aleatoric subpopulation

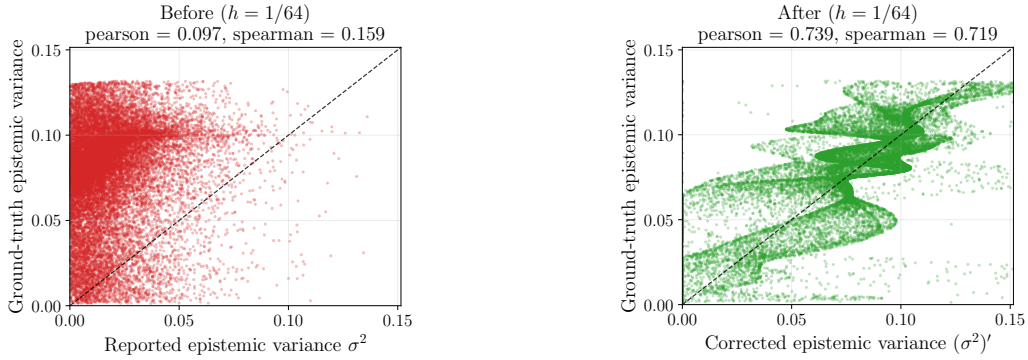


Figure 3: **Experiment 2 (recalibration)**. Reported  $\sigma^2$  (left) and corrected  $(\sigma^2)'$  (right) versus the ground-truth conditional variance on a held-out split, at  $h=1/64$ . Dashed line is  $y=x$ .

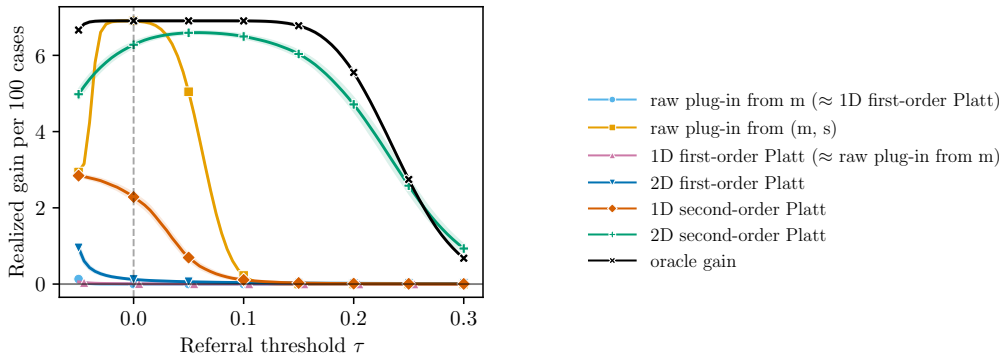


Figure 4: **Experiment 3 (decision utility)**. Realised gain per 100 borderline patients vs. referral threshold  $\tau$  (mean  $\pm 1.96$  SEM, 200 repeats). 2-D second-order Platt tracks the oracle; the raw  $(m, \sigma^2)$  plug-in collapses near  $\tau \approx 0.06$ .

( $\theta \approx 0.5$ , small  $\sigma^2$ ) and a hidden-subtype one ( $\theta \in \{0.12, 0.88\}$ , large  $\sigma^2$ ), both centred at  $m \approx 0.5$ . Figure 4 reports realised gain versus referral threshold  $\tau$ . 2-D second-order Platt tracks the oracle across the full  $\tau \geq 0$  range. The raw  $(m, \sigma^2)$  plug-in matches at  $\tau=0$  but *collapses* near  $\tau \approx 0.06$ : it ranks patients correctly but its score *magnitudes* are biased low on the epistemic group, so any cost-aware threshold drops the entire group. First-order methods cannot separate the subpopulations and refer essentially no one. The lesson is exactly what Proposition 3 promises and ranking-only metrics would hide: a calibrated  $\sigma^2$  matters numerically. App. B.3.

**Experiment 4 — the same effect on real labels.** We move to the public Weather Sentiment AMT dataset (300 tasks, 20 worker votes each, one-vs-rest binarisation), with an audit task whose downstream value provably depends on  $\eta_2$  and not just  $\eta_1$ : an auditor must rank items by the probability that two fresh workers disagree,  $g(\theta) = 2\theta(1 - \theta)$ , whose calibrated form  $2\eta_1(S) - 2\eta_2(S)$  requires  $\eta_2$ . Items are mixed in equal proportion from an aleatoric cohort ( $\theta \approx 1/2$ ) and a hidden-subtype cohort ( $\theta$  near 0 or 1); the score  $S = (m, s) \in [0, 1]^2$  is constructed in an XOR pattern so that the 1-D marginals of  $m$  and of  $s$  are *identical* between cohorts, leaving any 1-D calibrator information-theoretically blind. At a 5% audit budget, 2-D second-order Platt finds 46.4 disagreements per 100 audited items, versus 30.9 for 2-D first-order Platt,  $\sim 26$  for all four 1-D and raw baselines, and 49.8 for the oracle; the paired AUC lift of 2-D second-order over each non-oracle baseline has a 95% CI strictly above zero (per-baseline win fractions  $\geq 0.97$ ). On real labels, in a task whose value provably depends on  $\eta_2$ , second-order Platt is the only practical method that approaches the oracle. Full audit-yield curves and per-method statistics in App. B.4 (Fig. 5).

## 8 Related Work

**Higher-order calibration.** Ahdriz et al. [2025] introduced higher-order calibration via  $k$ -snapshots and a Wasserstein criterion defined over a partition of the score space, but provided no finite-sample estimation bounds. We dispense with the partition (Appendix D relates the two formulations quantitatively), give the first finite-sample bound for  $CE_2$ , and provide the first post-hoc method with a second-order guarantee. Ahdriz et al. [2025] also propose a bucketed analogue of Platt scaling, without data-efficiency bounds.

**First-order calibration measurement.** ECE is conventionally estimated by binning [Naeini et al., 2015, Guo et al., 2017], but binned estimators are biased and inconsistent [Vaicenavicius et al., 2019, Kumar et al., 2019]. Kumar et al. [2019] give a debiased estimator with finite-sample bounds, Roelofs et al. [2022] empirically compare variants, and Widmann et al. [2019] obtain consistent multi-class estimators via matrix-valued kernels. Błasiok et al. [2023] unify this literature through the distance to calibration, identifying which measures are polynomially related to it. Closest in spirit to our work is the SmoothECE of Błasiok and Nakkiran [2023], a first-order calibration measure built from Nadaraya–Watson regression with a reflected-Gaussian kernel. We differ in two essential respects: we target the two-dimensional second-order error  $CE_2$ , and we use the sech kernel of Ciosek et al. [2026], whose poles in the complex plane render the perturbed calibration functions *analytic* in a strip rather than merely smooth. Bernstein-ellipse approximation then yields exponential (rather than polynomial) polynomial-approximation rates, which is what lets us achieve  $\tilde{O}(1/\sqrt{n})$  in two dimensions where a Nadaraya–Watson analogue would give  $n^{-1/4}$ . Ciosek et al. [2026] themselves establish only an  $n^{-1/3}$  rate for the first-order error and do not exploit analyticity. Lee et al. [2023] study the complementary problem of *testing* first-order calibration and prove minimax optimality of their T-Cal procedure under a smoothness assumption.

**Distribution-free impossibility.** Gupta et al. [2020] prove that no scoring function whose level sets induce an uncountable partition of the input space admits a distribution-free asymptotic first-order calibration guarantee, ruling out continuous parametric recalibrators like Platt scaling and temperature scaling and leaving binning as the only route to a finite-sample bound. Our perturbation circumvents this impossibility as an inference-time design choice rather than an assumption on the data.

**Post-hoc calibration.** Platt scaling [Platt et al., 1999], isotonic regression [Zadrozny and Elkan, 2002], beta calibration [Kull et al., 2017], and temperature scaling [Guo et al., 2017] are the standard first-order recalibration methods: each fits a low-dimensional map from scores to corrected probabilities and inherits a calibration guarantee by construction (up to estimation error). Our second-order Platt scaling is, to our knowledge, the first post-hoc procedure that recalibrates both a mean prediction and an epistemic-variance estimate with provable finite-sample bounds on the calibration error of the recalibrated classifier.

**Multicalibration.** A complementary line of work strengthens first-order calibration along the subgroup axis rather than the moment axis. Hébert-Johnson et al. [2018] require the mean prediction to be calibrated simultaneously on every subpopulation in a rich, computationally-identifiable class. Our work is orthogonal: we calibrate the second moment on the predictor’s own level sets rather than the first moment across many subgroups. Combining the two ie. developing multicalibrated higher-order predictors is a natural direction left to future work.

**Additional Related Work** We provide additional pointers to related work in appendix A.

## 9 Conclusion

We have shown that the sech perturbation kernel, previously used to enforce smoothness of calibration functions, in fact makes them analytic. Exploiting this via polynomial regression yields near-parametric  $\tilde{O}(1/\sqrt{n})$  estimation of both calibration functions  $\eta_1$  and  $\eta_2$ , and hence of the second-order calibration error  $CE_2$ . Remapping the predictor through the estimated calibration functions produces a second-order calibrated predictor whose epistemic uncertainty has provable real-world semantics. We briefly explore remaining open questions in Appendix G.

## References

- Gustaf Ahdritz, Aravind Gollakota, Parikshit Gopalan, Charlotte Peale, and Udi Wieder. Provable uncertainty decomposition via higher-order calibration. In *The Thirteenth International Conference on Learning Representations*, 2025. URL <https://openreview.net/forum?id=TIId1SHe8JG>.
- Anastasios N Angelopoulos and Stephen Bates. Conformal prediction: A gentle introduction. *Foundations and Trends in Machine Learning*, 16(4):494–591, 2023.
- Peter Bartlett. Theoretical Statistics. Lecture 12, 2013. URL <https://www.stat.berkeley.edu/~bartlett/courses/2013spring-stat210b/notes/12notes.pdf>.
- Jarosław Błasiok and Preetum Nakkiran. Smooth ece: Principled reliability diagrams via kernel smoothing. *arXiv preprint arXiv:2309.12236*, 2023.
- Jarosław Błasiok, Parikshit Gopalan, Lunjia Hu, and Preetum Nakkiran. A unifying theory of distance from calibration. In *Proceedings of the 55th Annual ACM Symposium on Theory of Computing*, pages 1727–1740, 2023.
- Kamil Ciosek, Nicolò Felicioni, Sina Ghiassian, Juan Elenter, Francesco Tonolini, David Gustafsson, Eva Garcia-Martin, Carmen Barcena Gonzalez, and Raphaëlle Bertrand-Lalo. Measuring uncertainty calibration. In *The Fourteenth International Conference on Learning Representations*, 2026. URL <https://openreview.net/forum?id=4AjfwNnWAV>.
- Stefan Depeweg, Jose-Miguel Hernandez-Lobato, Finale Doshi-Velez, and Steffen Udluft. Decomposition of uncertainty in bayesian deep learning for efficient and risk-sensitive learning. In *International conference on machine learning*, pages 1184–1193. PMLR, 2018.
- H. Fawzi. Numerical Analysis – Lecture 13, 2023. URL <https://www.damtp.cam.ac.uk/user/hf323/M23-II-NA/Lect13.pdf>. Lecture Notes.
- Chuan Guo, Geoff Pleiss, Yu Sun, and Kilian Q Weinberger. On calibration of modern neural networks. In *International conference on machine learning*, pages 1321–1330. PMLR, 2017.
- Chirag Gupta, Aleksandr Podkopaev, and Aaditya Ramdas. Distribution-free binary classification: prediction sets, confidence intervals and calibration. *Advances in Neural Information Processing Systems*, 33:3711–3723, 2020.
- Ursula Hébert-Johnson, Michael Kim, Omer Reingold, and Guy Rothblum. Multicalibration: Calibration for the (computationally-identifiable) masses. In *International Conference on Machine Learning*, pages 1939–1948. PMLR, 2018.
- Paul Hofman, Yusuf Sale, and Eyke Hüllermeier. Quantifying aleatoric and epistemic uncertainty with proper scoring rules, 2024. URL <https://arxiv.org/abs/2404.12215>.
- Neil Houlsby, Ferenc Huszár, Zoubin Ghahramani, and Máté Lengyel. Bayesian active learning for classification and preference learning. *arXiv preprint arXiv:1112.5745*, 2011.
- Eyke Hüllermeier and Willem Waegeman. Aleatoric and epistemic uncertainty in machine learning: an introduction to concepts and methods. *Machine Learning*, 110:457 – 506, 2019. URL <https://api.semanticscholar.org/CorpusID:216465307>.
- Eyke Hüllermeier and Willem Waegeman. Aleatoric and epistemic uncertainty in machine learning: An introduction to concepts and methods. *Machine learning*, 110(3):457–506, 2021.
- Alex Kendall and Yarin Gal. What uncertainties do we need in bayesian deep learning for computer vision? *Advances in neural information processing systems*, 30, 2017.
- Meelis Kull, Telmo Silva Filho, and Peter Flach. Beta calibration: a well-founded and easily implemented improvement on logistic calibration for binary classifiers. In *Artificial intelligence and statistics*, pages 623–631. PMLR, 2017.
- Ananya Kumar, Percy S Liang, and Tengyu Ma. Verified uncertainty calibration. *Advances in neural information processing systems*, 32, 2019.

- Balaji Lakshminarayanan, Alexander Pritzel, and Charles Blundell. Simple and scalable predictive uncertainty estimation using deep ensembles. *Advances in neural information processing systems*, 30, 2017.
- Donghwan Lee, Xinneng Huang, Hamed Hassani, and Edgar Dobriban. T-cal: An optimal test for the calibration of predictive models. *Journal of Machine Learning Research*, 24(335):1–72, 2023.
- Andrey Malinin and Mark Gales. Predictive uncertainty estimation via prior networks. *Advances in neural information processing systems*, 31, 2018.
- Mahdi Pakdaman Naeini, Gregory Cooper, and Milos Hauskrecht. Obtaining well calibrated probabilities using bayesian binning. In *Proceedings of the AAAI conference on artificial intelligence*, volume 29, 2015.
- Ian Osband, Zheng Wen, Seyed Mohammad Asghari, Vikranth Dwaracherla, Morteza Ibrahimi, Xiuyuan Lu, and Benjamin Van Roy. Epistemic neural networks. *Advances in Neural Information Processing Systems*, 36:2795–2823, 2023.
- John Platt et al. Probabilistic outputs for support vector machines and comparisons to regularized likelihood methods. *Advances in large margin classifiers*, 10(3):61–74, 1999.
- Yury Polyanskiy and Yihong Wu. *Information Theory: From Coding to Learning*. Cambridge University Press, 2025.
- Patrick Rebeschini. Bernstein’s Concentration Inequalities. Fast Rates, 2021. URL <https://www.stats.ox.ac.uk/~rebesch/teaching/AFoL/22/material/lecture07.pdf>. Lecture Notes.
- Rebecca Roelofs, Nicholas Cain, Jonathon Shlens, and Michael C Mozer. Mitigating bias in calibration error estimation. In *International Conference on Artificial Intelligence and Statistics*, pages 4036–4054. PMLR, 2022.
- Yusuf Sale, Viktor Bengs, Michele Caprio, and Eyke Hüllermeier. Second-order uncertainty quantification: A distance-based approach. *arXiv preprint arXiv:2312.00995*, 2023.
- Yusuf Sale, Alireza Javanmardi, and Eyke Hüllermeier. Aleatoric and epistemic uncertainty in conformal prediction. 2025.
- Murat Sensoy, Lance Kaplan, and Melih Kandemir. Evidential deep learning to quantify classification uncertainty. *Advances in neural information processing systems*, 31, 2018.
- Juozas Vaicenavicius, David Widmann, Carl Andersson, Fredrik Lindsten, Jacob Roll, and Thomas Schön. Evaluating model calibration in classification. In *The 22nd international conference on artificial intelligence and statistics*, pages 3459–3467. PMLR, 2019.
- Vladimir Vovk, Alexander Gammerman, and Glenn Shafer. *Algorithmic learning in a random world*. Springer, 2005.
- David Widmann, Fredrik Lindsten, and Dave Zachariah. Calibration tests in multi-class classification: A unifying framework. *Advances in neural information processing systems*, 32, 2019.
- Lisa Wimmer, Yusuf Sale, Paul Hofman, Bernd Bischl, and Eyke Hüllermeier. Quantifying aleatoric and epistemic uncertainty in machine learning: Are conditional entropy and mutual information appropriate measures? In *Uncertainty in artificial intelligence*, pages 2282–2292. PMLR, 2023.
- Bianca Zadrozny and Charles Elkan. Transforming classifier scores into accurate multiclass probability estimates. In *Proceedings of the eighth ACM SIGKDD international conference on Knowledge discovery and data mining*, pages 694–699, 2002.

## A Further Related Work

**Second-order uncertainty measures.** A complementary line of work asks *what* second-order quantity ought to be measured, rather than how to calibrate it. Wimmer et al. [2023] examine entropy-based decompositions of aleatoric and epistemic uncertainty, Sale et al. [2023] propose Wasserstein-based alternatives, and Hofman et al. [2024] develop scoring-rule decompositions. These works concern what to measure; ours concerns how to calibrate it. The general aleatoric/epistemic distinction we exploit is reviewed in Hüllermeier and Waegeman [2021] and Hüllermeier and Waegeman [2019].

**Bayesian and evidential uncertainty decomposition.** Several lines of work produce mean-and-uncertainty outputs without calibration guarantees: Bayesian active learning by disagreement [Houlsby et al., 2011], variance decompositions for Bayesian neural networks [Depeweg et al., 2018, Kendall and Gal, 2017], and deep ensembles [Lakshminarayanan et al., 2017]. A complementary family bypasses ensembling by directly parameterising a higher-order output distribution: prior networks [Malinin and Gales, 2018] and evidential deep learning [Sensoy et al., 2018] both place a Dirichlet on the simplex and read epistemic uncertainty from its concentration. Second-order Platt scaling is agnostic to the source of  $(m, \sigma^2)$ : it can recalibrate the output of any of these methods post hoc.

**Distribution-free uncertainty quantification.** Our analysis is distribution-free in the sense that no assumption is placed on  $f^*$  or on the marginal of  $X$ ; the only structural input is the sech perturbation, which is a deployment-side design choice rather than an assumption on the data. A different distribution-free paradigm is conformal prediction [Vovk et al., 2005, Angelopoulos and Bates, 2023], which produces per-sample prediction sets with a marginal coverage guarantee on the label. Conformal set size reflects total predictive uncertainty and does not, on its own, separate aleatoric from epistemic components; recent work that attempts such a split [Sale et al., 2025] does so by importing an external decomposition and using conformal machinery to calibrate it. Second-order Platt scaling is complementary: it targets the moments of the conditional label distribution on the predictor’s level sets, yielding a calibrated epistemic-uncertainty scalar rather than a coverage-valid set.

## B Details of Experiments

### B.1 Experiment 1: Additional Details

**DGP and predictor.**  $X \in \mathbb{R}^4$  is drawn from a 10-component isotropic Gaussian mixture (centres  $\sim \mathcal{N}(0, 1.5^2 I)$ , unit-variance components);  $f^*(x) = \sigma(w^\top x)$  with  $w \sim \mathcal{N}(0, I/2)$ . The predictor is a 5-member MLP ensemble ( $4 \rightarrow 64 \rightarrow 64 \rightarrow 1$ , ReLU, BCE, Adam at  $10^{-3}$ , 30 epochs, batch 256) trained once on a fresh sample of 5,000; the score is its mean and unbiased variance, clipped to the feasible region. Independent truncated-sech perturbations on  $[0, 1]$  and  $[0, 1/4]$  are sampled in closed form via  $G^{-1}(u; s, h) = s + 2h \arctanh(\tan(u/(2h)))$ .

**Ground truth.** For each  $h$ ,  $\text{CE}_2^{\text{pert}}$  is computed by depositing a scrambled-Sobol QMC sample of size  $2^{18}$  on a  $1025 \times 257$  tensor grid, applying the truncated-sech kernel matrices exactly, and integrating the pointwise loss against the perturbed-score density (trapezoidal rule). Two independent Sobol replicates agree to  $\leq 2 \cdot 10^{-5}$ , much smaller than any estimator error.

**Baselines.** All estimators target  $\eta_1$  by regressing  $Y^{(1)}$  on the perturbed score and  $\eta_2$  by regressing  $Y^{(1)}Y^{(2)}$ . *Bucketing* uses  $K \times K$  axis-aligned cells with  $K = \text{clip}(\lceil c(n/h^2)^{1/4} \rceil, 2, 200)$ , the standard 2D-histogram MSE balance for an  $O(1/h)$ -Lipschitz target. *Nadaraya–Watson* uses an isotropic Gaussian kernel (truncated at  $5b$ ) of bandwidth  $b = ch^{1/2}n^{-1/4}$  on the  $\sigma^2$ -rescaled rectangle (multiplying  $\sigma^2$  by 4 so both axes have unit support). The constant  $c$  is selected from  $\{0.25, 0.5, 1, 2, 4, 8\}$  on a held-out split by squared-error loss; bucketing dyadically extends the grid if the optimum lies on the boundary.

**Polynomial estimator.** Tensor Chebyshev features of degree  $l$  per axis, fit by ridge with  $\lambda$  scaled by  $\text{tr}(G)/d$ , switching to dual form when  $(l + 1)^2 > n$ . The candidate degree schedule starts at  $l_{\max} =$

$\min(l_{\text{paper}}, L_{\text{cap}})$  with  $l_{\text{paper}}(n, h) = \lceil 2 \log n / \log \theta(h) \rceil$  (the analytic choice from Proposition 1) and per- $h$  caps  $L_{\text{cap}} \in \{44, 88\}$  for  $h \in \{1/16, 1/64\}$ , then halves down to a floor of 4. The ridge multiplier is selected from  $\{10^{-6}, \dots, 1\}$ . *val*:  $(l, \alpha)$  chosen on a held-out hyper split. *ERM, CV*: 5-fold CV on the validation split, with closed-form leave-one-out predictions reported on the same split. Per-coordinate predictions clipped to  $[0, 1]$ .

**Sampling and aggregation.** For each of 20 seeds we draw three i.i.d. splits (train, hyper, valid) of size 50,000; perturbations are redrawn per  $h$ , raw scores and labels are shared across  $h$ . For each  $n \in \{500, 10^3, 2 \cdot 10^3, 5 \cdot 10^3, 10^4, 2 \cdot 10^4, 5 \cdot 10^4\}$  the estimators use only the first  $n$  samples of each split (so per-seed  $n$ -curves are coupled). Bands are Student- $t$  90% intervals across seeds; reported slopes are least-squares fits in  $\log_{10}(n)$  vs.  $\log_{10}(\text{mean error})$ .

## B.2 Experiment 2: implementation details

**Ensemble.** 20 MLPs (4-64-64-1, ReLU), each trained for 60 epochs of BCE with Adam (lr  $10^{-3}$ , batch 256) on the same 24  $(x, y)$  pairs from the DGP, varying only the initialisation seed. The small per-member training set keeps the disagreement variance informative. Outputs are clipped to the feasible set  $\sigma^2 \leq m(1-m)$ .

**Ground-truth surfaces.** For each  $h$ , we draw  $2^{18}$  scrambled Sobol points from the DGP and bilinearly deposit  $(1, p, p^2)$  on a  $1025 \times 257$  tensor grid over  $[0, 1] \times [0, 1/4]$ . Convolution each axis with the 1D sech kernel at bandwidth  $h$  yields gridded  $\eta_1, \eta_2$  and a perturbed score density; the ground-truth conditional variance and  $\text{CE}_2$  at  $h$  are read off these surfaces, with bilinear interpolation at arbitrary perturbed scores.

**Recalibrator.**  $(M, \Sigma)$  is affinely mapped to  $[-1, 1]^2$  and lifted to a tensor-Chebyshev basis of degree 12 (169 features). The two regressions for  $\hat{\eta}_1, \hat{\eta}_2$  share this basis and are solved by Cholesky on the  $169 \times 169$  Gram matrix, with only a numerical ridge floor of  $10^{-12} \cdot \text{tr}(G)/169$  (no cross-validation, no degree search). Predictions are projected onto the feasible moment region  $\hat{\eta}_1 \in [0, 1], \hat{\eta}_2 \in [\hat{\eta}_1^2, \hat{\eta}_1]$  before forming  $(\sigma^2)'$ .

**Variance across seeds.** The  $\text{CE}_2$  intervals reported in the main text are mean  $\pm$  standard deviation over 20 independent draws of the  $n=2 \cdot 10^4$  calibration set.

## B.3 Experiment 3 details

**DGP.** Four-group mixture with weights  $(0.25, 0.25, 0.35, 0.15)$ . Groups 0/1 are clear negatives/positives concentrated at  $\theta \approx 0.08$  and  $\theta \approx 0.92$  (small  $\sigma^2$ ); they contribute negligible mass after the borderline filter and exist only so the unfiltered population has full support over  $m$ . The two groups that populate the borderline cohort:

- *Group 2 (aleatoric, weight 0.35):*  $m \sim \mathcal{N}(0.5, 0.035^2)$ ,  $\sigma^2 \sim \mathcal{N}(0.010, 0.002^2)$ ,  $\theta \sim \mathcal{N}(0.5, 0.040^2)$ .
- *Group 3 (hidden subtype, weight 0.15):*  $m \sim \mathcal{N}(0.5, 0.035^2)$ ,  $\sigma^2 \sim \mathcal{N}(0.060, 0.010^2)$ ; subtype  $b \sim \text{Unif}\{0, 1\}$ , then  $\theta \sim \mathcal{N}(0.12, 0.030^2)$  if  $b = 0$ , else  $\mathcal{N}(0.88, 0.030^2)$ .

All draws are independently clipped so that  $m, \theta \in [0, 1]$  and  $\sigma^2 \in [0, 1/4]$ . Within the borderline cohort,  $\eta_1 \approx 0.5$  for both groups while  $\eta_2 \approx 0.25$  versus  $\eta_2 \approx 0.5$ , so the two cannot be separated from  $m$  alone.

**Calibrators.** Tensor-product Chebyshev features  $(T_0, \dots, T_d)$  on  $2m-1 \in [-1, 1]$  and on  $8\sigma^2-1 \in [-1, 1]$  with  $d_{1D} = 6$  and per-axis  $d_{2D} = 4$  (25 features), fit by ridge ERM with ridge  $10^{-4}$ . Calibration labels are 2-snapshots  $Y^{(1)}, Y^{(2)} \stackrel{\text{iid}}{\sim} \text{Bernoulli}(\theta)$ ; first-order calibrators regress  $Y^{(1)}$  and set  $\hat{\eta}_2 := \hat{\eta}_1^2$ , second-order calibrators jointly regress  $(Y^{(1)}, Y^{(1)}Y^{(2)})$ . Predicted moments are projected onto  $\{\hat{\eta}_1 \in [0, 1], \hat{\eta}_1^2 \leq \hat{\eta}_2 \leq \hat{\eta}_1\}$  (Jensen plus the Bernoulli upper bound  $\theta^2 \leq \theta$ ). Each method's patient score is  $2\hat{\eta}_2 - 2\hat{\eta}_1 + 0.5 - c$ .

**Methods.** Seven curves in Figure 4: (i) raw plug-in from  $m$  ( $\hat{\eta}_1 := m, \hat{\eta}_2 := m^2$ ); (ii) raw plug-in from  $(m, \sigma^2)$  ( $\hat{\eta}_1 := m, \hat{\eta}_2 := m^2 + \sigma^2$ , then project); (iii)/(iv) 1D/2D first-order Platt; (v)/(vi) 1D/2D second-order Platt; (vii) oracle, scoring with the true  $\theta$ .

**Replication.** 200 independent repeats with seeds  $0, \dots, 199$ ; pre-filter sizes  $N_{\text{cal}} = 3000, N_{\text{eval}} = 8000$  (about half pass the borderline filter under the group weights); threshold grid of 71 points in  $[-0.05, 0.30]$ . Bands in Fig. 4 are  $\pm 1.96$  SEM across repeats. We did not tune the polynomial degrees, ridge, or filter range; the values above were our first choice. Source code is included with the submission.

#### B.4 Experiment 4: details

**Data.** Weather Sentiment AMT: per-(worker, task) categorical responses with majority-vote gold. We binarise as one-vs-rest on the gold class; the figure uses class 1. Tasks with fewer than 5 votes are dropped, leaving 300 tasks with 20 votes each.

**Cohort, provisional label, and  $\theta$ .** Let  $\hat{p}_i$  be the empirical positive rate of the binary votes for item  $i$ . The aleatoric cohort is  $\{i : |\hat{p}_i - \frac{1}{2}| \leq 0.22\}$ , the hidden-subtype cohort is  $\{i : \hat{p}_i \leq 0.12 \text{ or } \hat{p}_i \geq 0.88\}$ , and the two are balanced to equal size. Each item is assigned a provisional binary label  $\text{prov}_i$ : aleatoric items use  $\text{Bernoulli}(\frac{1}{2})$ ; hidden items use the empirical majority for half (chosen uniformly) and its complement for the other half. The agreement probability of a fresh worker is then  $\theta_i = \hat{p}_i$  if  $\text{prov}_i = 1$ , else  $1 - \hat{p}_i$ . Aleatoric items therefore have  $\theta_i \approx \frac{1}{2}$ , hidden items  $\theta_i$  near 0 or 1; both cohorts have  $\mathbb{E}\theta_i \approx \frac{1}{2}$  but very different  $\mathbb{E}\theta_i^2$ .

**Score construction (XOR mode).** Let  $\text{lo} = \frac{1}{2} - s_{\text{gap}}/2, \text{hi} = \frac{1}{2} + s_{\text{gap}}/2$  with  $s_{\text{gap}} = 0.35$ . Draw  $b_i \sim \text{Bernoulli}(\frac{1}{2})$  and set  $m_i = \text{hi}$  if  $b_i = 1$  else  $\text{lo}$ ; set  $s_i = \text{hi}$  if  $\mathbb{1}[\text{kind}_i = \text{aleatoric}] = b_i$ , else  $\text{lo}$ . Add independent Gaussian noise of std  $\sigma_m = 0.06, \sigma_s = 0.08$  and clip to  $[0, 1]$ . By construction the marginal of  $m$  and the marginal of  $s$  are the same Gaussian-noisy two-mode mixture in both cohorts, while the joint pattern is a cohort-aligned XOR.

**Calibrators.** For each calibration item,  $\hat{\eta}_1$  is fit to  $a_i/n_i$  and  $\hat{\eta}_2$  to  $a_i(a_i - 1)/(n_i(n_i - 1))$ , the unbiased all-pairs estimators of  $\theta_i$  and  $\theta_i^2$ . Feature maps: 1-D is  $[1, m, \dots, m^4]$ ; 2-D is the total-degree-3 tensor basis in  $(m, s)$ , 10 features. We use ridge regression with  $\lambda = 10^{-3}$ . Predictions are clipped to  $\hat{\eta}_1 \in [0, 1]$  and projected to the admissible region  $\hat{\eta}_1^2 \leq \hat{\eta}_2 \leq \hat{\eta}_1$ .

**Methods.** Eight ranking scores: raw  $2m(1 - m)$ ; raw  $s$ ; raw  $1 - s$ ; 1-D first-order  $2\hat{\eta}_1^{1D}(1 - \hat{\eta}_1^{1D})$ ; 1-D second-order  $2\hat{\eta}_1^{1D} - 2\hat{\eta}_2^{1D}$ ; 2-D first-order  $2\hat{\eta}_1^{2D}(1 - \hat{\eta}_1^{2D})$ ; 2-D second-order  $2\hat{\eta}_1^{2D} - 2\hat{\eta}_2^{2D}$  (primary); oracle  $g(\theta_i) = 2\theta_i(1 - \theta_i)$ , shown for upper-bound reference only.

**Splits and reporting.** Per repeat, items are partitioned disjointly into selection (25%), calibration (35%), evaluation (rest). Cohort thresholds,  $s_{\text{gap}}$ , noise scales, score-mode, and target class are chosen on the selection split by a held-out audit-AUC lift criterion; the final figure uses 1000 fresh draws of the calibration/evaluation split at the chosen configuration ( $\text{extreme\_thr}, \text{ale\_width}, \sigma_m, \sigma_s, s_{\text{gap}}$ ) =  $(0.12, 0.22, 0.06, 0.08, 0.35)$ . Yield at audit fraction  $f$  is  $100 \cdot \overline{g(\theta_i)}$  over the top- $\lceil fn_{\text{ev}} \rceil$  evaluation items by score; bands are  $\pm 1.96$  SEM across repeats. Source code reproducing all numbers and figures is included with the submission.

**Per-method audit-yield summary.** At a 5% audit budget the seven non-oracle methods are well separated into three tiers: 2-D second-order Platt at 46.4 disagreements per 100 audited items; 2-D first-order Platt at 30.9; and the four 1-D and raw baselines (raw  $m$ , raw  $s$ , raw  $1 - s$ , 1-D first-order, 1-D second-order) clustered around  $\sim 26$ . The oracle  $g(\theta_i) = 2\theta_i(1 - \theta_i)$  achieves 49.8. The paired AUC lift of 2-D second-order Platt over each of the six non-oracle baselines has a 95% CI strictly above zero, with per-baseline win fractions  $\geq 0.97$  across the 1000 evaluation repeats — i.e., the 2-D-second-order ordering audit-AUC dominates each baseline’s ordering on essentially every draw, not just on average. The collapse of all 1-D and raw curves onto a common envelope is expected by construction: the XOR score design makes the cohort indicator information-theoretically unrecoverable from any single coordinate, so no 1-D calibrator can do better than chance at distinguishing aleatoric from hidden-subtype items.

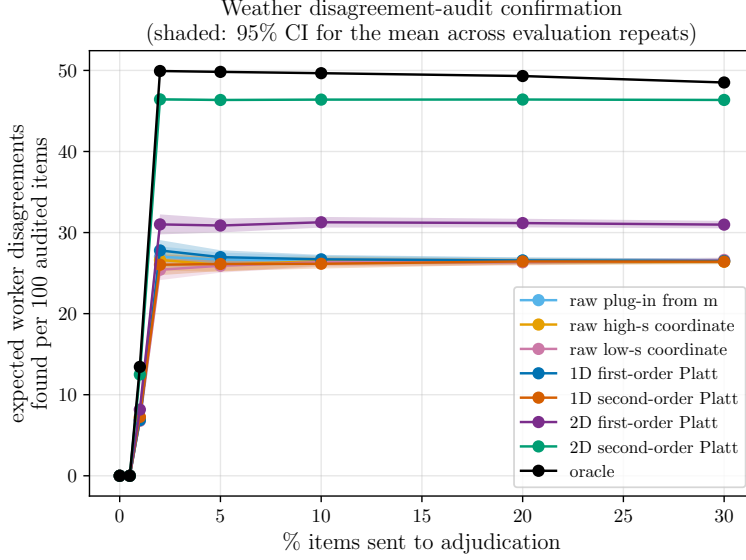


Figure 5: **Experiment 4: full audit-yield curves.** Yield (expected fresh-worker disagreements found per 100 audited items) vs. audit budget on the Weather Sentiment AMT cohort, over 1000 evaluation repeats. 2-D second-order Platt is the only non-oracle method that exploits the joint  $(m, s)$  structure required by the decision problem; all 1-D and raw baselines collapse onto a common curve because the 1-D marginals are identical between the aleatoric and hidden-subtype cohorts by construction. Bands are  $\pm 1.96$  SEM.

## C Proofs

### C.1 Auxiliary lemma

**Lemma 3** (Positive real part). *For any  $a \in \mathbb{R}$  and  $|b| < \pi/2$ :*

$$\operatorname{Re}(\operatorname{sech}(a + ib)) = \frac{\cosh(a) \cos(b)}{|\cosh(a + ib)|^2} > 0.$$

*Proof.*  $\cosh(a + ib) = \cosh(a) \cos(b) + i \sinh(a) \sin(b)$ . So

$$\operatorname{Re}(1/\cosh(a + ib)) = \operatorname{Re}(\overline{\cosh(a + ib)})/|\cosh(a + ib)|^2 = \cosh(a) \cos(b)/|\cosh(a + ib)|^2.$$

Since  $\cosh(a) > 0$  for all real  $a$  and  $\cos(b) > 0$  for  $|b| < \pi/2$ , the result follows.  $\square$

### C.2 Proof of analyticity of calibration functions (lemma 1)

*Proof.* We give the argument for  $\eta_1$  in 1D; the 2D case follows by applying the same argument in each variable.

The perturbed calibration function is  $\eta_1(t) = N(t)/D(t)$  (see appendix D.1.1 of the work by Ciosek et al. [2026]). Here

$$N(t) = \int_0^1 \eta_1^{\text{orig}}(s) \tilde{p}(s) \operatorname{sech}\left(\frac{t-s}{h}\right) ds, \quad (13)$$

$$D(t) = \int_0^1 \tilde{p}(s) \operatorname{sech}\left(\frac{t-s}{h}\right) ds, \quad (14)$$

and  $\tilde{p}(s) = p_S(s)/Z(s, h) \geq 0$  absorbs the score density  $p_S$  and the normalizer  $Z$ .

**Analyticity of  $N$  and  $D$ .** For each fixed  $s \in [0, 1]$ , the function  $z \mapsto \operatorname{sech}((z - s)/h)$  is analytic in  $|\operatorname{Im}(z)| < h\pi/2$  (since  $\operatorname{sech}(w) = 1/\cosh(w)$  has its nearest poles at  $w = \pm i\pi/2$ , i.e., at  $z = s \pm ih\pi/2$ ). Moreover, for  $z = t + ib$  with  $t \in [0, 1]$  and  $|b| \leq h\pi/2 - \delta$  (any  $\delta > 0$ ):

$$|\operatorname{sech}((z - s)/h)| = \frac{1}{|\cosh((t - s)/h + ib/h)|} \leq \frac{1}{\cos(b/h) \cdot 1} \leq \frac{1}{\cos(\pi/2 - \delta/h)},$$

which is a uniform bound in  $s$  and  $t$ . Since the integrand  $\eta_1^{\operatorname{orig}}(s)\tilde{p}(s)\operatorname{sech}((z - s)/h)$  is bounded uniformly on the compact domain  $s \in [0, 1]$  for  $z$  in any compact subset of the strip, differentiation under the integral is justified by dominated convergence. Therefore  $N(z)$  and  $D(z)$  are analytic in the strip.

**Non-vanishing of  $D$ .** For  $z = t + ib$  with  $|b| < h\pi/2$ :

$$\operatorname{Re}(D(t + ib)) = \int_0^1 \tilde{p}(s) \operatorname{Re}\left(\operatorname{sech}\left(\frac{t + ib - s}{h}\right)\right) ds > 0,$$

by Lemma 3: the integrand  $\tilde{p}(s) \cdot \operatorname{Re}(\operatorname{sech}(\dots))$  is non-negative (since  $\tilde{p} \geq 0$  and  $\operatorname{Re}(\operatorname{sech}) > 0$ ) and not identically zero (since  $\tilde{p}$  has positive mass). Therefore  $D(z) \neq 0$  in the strip, and  $\eta_1 = N/D$  is analytic there.

**2D extension.** For the product perturbation on  $\mathcal{R} = [0, 1] \times [0, \frac{1}{4}]$ :

$$D(\tilde{m}, \tilde{\sigma}^2) = \iint_{\mathcal{F}} \tilde{p}(m, \sigma^2) \operatorname{sech}\left(\frac{\tilde{m} - m}{h}\right) \operatorname{sech}\left(\frac{\tilde{\sigma}^2 - \sigma^2}{h}\right) d\sigma^2 dm.$$

For fixed real  $\tilde{\sigma}^2 = c$ , the inner integral  $g(m) = \int \tilde{p}(m, \sigma^2) \operatorname{sech}((c - \sigma^2)/h) d\sigma^2 \geq 0$  is a non-negative weight (with  $\operatorname{sech}$  real and positive for real arguments). Then  $D(\tilde{m}, c) = \int g(m) \operatorname{sech}((\tilde{m} - m)/h) dm$ , and the 1D argument above shows  $D \neq 0$  in  $|\operatorname{Im}(\tilde{m})| < h\pi/2$ . The same argument applies in the other variable. By Hartogs' theorem, separate analyticity implies joint analyticity.  $\square$

### C.3 Bernstein Ellipse Theorem in our notation (lemma 2 in main text)

*Proof.* Define

$$g(x) := f\left(\frac{x + 1}{2}\right), \quad x \in [-1, 1].$$

Since  $f$  is analytic in the strip

$$\{z \in \mathbb{C} : |\operatorname{Im}(z)| < \rho\},$$

the function  $g$  is analytic in the strip

$$S := \{x \in \mathbb{C} : |\operatorname{Im}(x)| < 2\rho\},$$

because

$$\operatorname{Im}\left(\frac{x + 1}{2}\right) = \frac{\operatorname{Im}(x)}{2},$$

so  $x \in S$  implies

$$\left|\operatorname{Im}\left(\frac{x + 1}{2}\right)\right| < \rho.$$

Moreover,  $|g(x)| \leq M$  on  $S$ .

Now let  $B(a)$  be the Bernstein ellipse from Theorem 3.17 of the lecture notes by Fawzi [2023]:

$$B(a) = \left\{x + iy \in \mathbb{C} : \frac{x^2}{\cosh^2(a\pi)} + \frac{y^2}{\sinh^2(a\pi)} < 1\right\}.$$

If  $z = x + iy \in B(a)$ , then

$$\frac{y^2}{\sinh^2(a\pi)} < 1,$$

hence

$$|\operatorname{Im}(z)| = |y| < \sinh(a\pi).$$

Choose  $a > 0$  so that

$$\sinh(a\pi) = 2\rho.$$

Then every  $z \in B(a)$  satisfies

$$|\operatorname{Im}(z)| < 2\rho,$$

so

$$B(a) \subset S.$$

Therefore  $g$  is analytic on  $B(a)$  and satisfies

$$\sup_{z \in B(a)} |g(z)| \leq M.$$

By the Bernstein ellipse Theorem [Fawzi, 2023, Theorem 3.17], for every  $l \geq 0$  there exists a polynomial  $p_l$  of degree  $l$  such that

$$\sup_{x \in [-1, 1]} |g(x) - p_l(x)| \leq 2M \frac{c^{l+1}}{1-c}, \quad c = e^{-a\pi}.$$

Now define

$$q_l(t) := p_l(2t - 1), \quad t \in [0, 1].$$

Then  $q_l$  is a polynomial of degree  $l$ , and with  $x = 2t - 1$ ,

$$\sup_{t \in [0, 1]} |f(t) - q_l(t)| = \sup_{x \in [-1, 1]} |g(x) - p_l(x)|.$$

Finally, set  $\theta := e^{a\pi}$ . Since  $\sinh(a\pi) = 2\rho$ , we have

$$\theta = e^{a\pi} = \sinh(a\pi) + \sqrt{1 + \sinh^2(a\pi)} = 2\rho + \sqrt{4\rho^2 + 1},$$

and therefore  $c = \theta^{-1}$ . Hence

$$2M \frac{c^{l+1}}{1-c} = 2M \frac{\theta^{-(l+1)}}{1-\theta^{-1}} = 2M \frac{\theta^{-l}}{\theta-1}.$$

This proves the claim. □

#### C.4 Covering Number Lemma

**Lemma 4.** *Let*

$$\mathcal{P}_l := \left\{ p(x, y) = \sum_{i=0}^l \sum_{j=0}^l a_{ij} x^i y^j : \|p\|_\infty \leq 1 \right\},$$

where

$$\|p\|_\infty := \sup_{(x, y) \in [0, 1]^2} |p(x, y)|.$$

Then for every  $0 < \varepsilon \leq 1$ ,

$$N(\varepsilon, \mathcal{P}_l, \|\cdot\|_\infty) \leq \left( \frac{3}{\varepsilon} \right)^{(l+1)^2}.$$

Equivalently,

$$\log N(\varepsilon, \mathcal{P}_l, \|\cdot\|_\infty) \leq (l+1)^2 \log \left( \frac{3}{\varepsilon} \right).$$

*Proof.* Let

$$V_m := \text{span}\{x^i y^j : 0 \leq i, j \leq l\}.$$

Then  $V_m$  is a linear space of dimension

$$d = (l + 1)^2,$$

since the monomials  $\{x^i y^j : 0 \leq i, j \leq l\}$  form a basis.

Equip  $V_m$  with the norm  $\|\cdot\|_\infty$ . By definition,  $\mathcal{P}_l$  is contained in the unit ball

$$B := \{p \in V_l : \|p\|_\infty \leq 1\}$$

of the  $d$ -dimensional normed space  $(V_l, \|\cdot\|_\infty)$ . Hence

$$N(\varepsilon, \mathcal{P}_l, \|\cdot\|_\infty) \leq N(\varepsilon, B, \|\cdot\|_\infty).$$

Now apply the standard volumetric bound for the unit ball of a  $d$ -dimensional normed space [Bartlett, 2013, Slide 7]:

$$N(\varepsilon, B, \|\cdot\|_\infty) \leq \left(1 + \frac{2}{\varepsilon}\right)^d.$$

Since  $0 < \varepsilon \leq 1$ ,

$$1 + \frac{2}{\varepsilon} \leq \frac{3}{\varepsilon}.$$

Therefore

$$N(\varepsilon, \mathcal{P}_l, \|\cdot\|_\infty) \leq \left(\frac{3}{\varepsilon}\right)^d = \left(\frac{3}{\varepsilon}\right)^{(l+1)^2}.$$

Taking logarithms gives

$$\log N(\varepsilon, \mathcal{P}_l, \|\cdot\|_\infty) \leq (l + 1)^2 \log\left(\frac{3}{\varepsilon}\right).$$

□

## C.5 More Auxiliary Lemmas

**Lemma 5.** *We have*

$$\mathbb{E}[h_f] \leq 4\varepsilon_l^2 + \frac{406 d \log(3n) + 408}{n}.$$

*Proof.* To keep constants explicit, we use the covering bound from lemma 4 in the form

$$N(\delta, \mathcal{P}_l, \|\cdot\|_\infty) \leq \left(\frac{3}{\delta}\right)^d, \quad 0 < \delta \leq 1,$$

with  $d = (l + 1)^2$ .

Set

$$\delta_n := \frac{1}{n},$$

and let  $\mathcal{G}_n \subset \mathcal{P}_l$  be a  $\delta_n$ -cover of  $\mathcal{P}_l$  in  $\|\cdot\|_\infty$ . Then

$$|\mathcal{G}_n| \leq N(\delta_n, \mathcal{P}_l, \|\cdot\|_\infty) \leq (3n)^d.$$

For every  $f \in \mathcal{P}_l$ , choose  $g_f \in \mathcal{G}_n$  such that

$$\|f - g_f\|_\infty \leq \delta_n.$$

Recall that

$$h_f(S, Z) = (f(S) - Z)^2 - (f^*(S) - Z)^2.$$

If  $f, g \in \mathcal{P}_l$ , then

$$h_f - h_g = (f - g)(f + g - 2Z),$$

hence, since  $f, g \in [0, 1]$  and  $Z \in \{0, 1\}$ ,

$$|h_f - h_g| \leq 2|f - g| \leq 2\|f - g\|_\infty.$$

Therefore

$$|Ph_f - Ph_g| \leq 2\|f - g\|_\infty, \quad |P_n h_f - P_n h_g| \leq 2\|f - g\|_\infty,$$

where  $P_n h := \frac{1}{n} \sum_{i=1}^n h(S_i, Z_i)$ . In particular, for the ERM  $\hat{f}$ , since  $P_n h_{\hat{f}} \leq 0$ ,

$$P_n h_{g_{\hat{f}}} \leq P_n h_{\hat{f}} + 2\delta_n \leq \frac{2}{n},$$

and

$$Ph_{\hat{f}} \leq Ph_{g_{\hat{f}}} + 2\delta_n.$$

Now fix  $g \in \mathcal{G}_n$ , and write

$$\mu_g := Ph_g = \mathbb{E}[h_g].$$

By Step 2(b),  $h_g \in [-4, 4]$ , so

$$(\mu_g - h_g) \leq \mu_g + 4 \leq 8.$$

Applying Bernstein's inequality [Rebeschini, 2021, Corollary 7.3] to the random variables

$$X_i := \mu_g - h_g(S_i, Z_i),$$

which satisfy  $X_i - \mathbb{E}X_i \leq 8$ , gives for every  $t > 0$ ,

$$\Pr(\mu_g - P_n h_g \geq t) \leq \exp\left(-\frac{nt^2}{2(\text{Var}(h_g) + \frac{8}{3}t)}\right).$$

By Step 2(c),

$$\text{Var}(h_g) \leq \mathbb{E}[h_g^2] \leq 32\mu_g + 64\varepsilon_l^2.$$

Hence

$$\Pr(\mu_g - P_n h_g \geq t) \leq \exp\left(-\frac{nt^2}{2(32\mu_g + 64\varepsilon_l^2 + \frac{8}{3}t)}\right).$$

Suppose now that

$$\mu_g \geq \frac{4}{n} \quad \text{and} \quad \mu_g \geq 4\varepsilon_l^2.$$

Then  $t := \mu_g - \frac{2}{n}$  satisfies  $t \geq \mu_g/2$ , and therefore

$$\Pr\left(P_n h_g \leq \frac{2}{n}\right) \leq \exp\left(-\frac{n(\mu_g/2)^2}{2(32\mu_g + 64\varepsilon_l^2 + \frac{8}{3}\mu_g)}\right).$$

Using  $64\varepsilon_l^2 \leq 16\mu_g$ , the denominator is at most

$$2\left(32\mu_g + 16\mu_g + \frac{8}{3}\mu_g\right) = \frac{304}{3}\mu_g,$$

so

$$\Pr\left(P_n h_g \leq \frac{2}{n}\right) \leq \exp\left(-\frac{3n\mu_g}{1216}\right) \leq \exp\left(-\frac{n\mu_g}{406}\right).$$

Now fix  $u \geq 0$ , and define

$$r(u) := \max\left\{\frac{4}{n}, 4\varepsilon_l^2, \frac{406(d \log(3n) + u)}{n}\right\}.$$

If  $\mu_g \geq r(u)$ , then

$$\Pr\left(P_n h_g \leq \frac{2}{n}\right) \leq \exp\left(-\frac{nr(u)}{406}\right) \leq \exp(-d \log(3n) - u) = (3n)^{-d} e^{-u}.$$

Taking a union bound over all  $g \in \mathcal{G}_n$ , and using  $|\mathcal{G}_n| \leq (3n)^d$ , we obtain

$$\Pr\left(\exists g \in \mathcal{G}_n : Ph_g \geq r(u) \text{ and } P_n h_g \leq \frac{2}{n}\right) \leq e^{-u}.$$

On the complementary event, the particular net point  $g_{\hat{f}}$  associated with  $\hat{f}$  cannot satisfy  $Ph_{g_{\hat{f}}} \geq r(u)$ , because we already know  $P_n h_{g_{\hat{f}}} \leq 2/n$ . Thus

$$Ph_{g_{\hat{f}}} < r(u),$$

and hence

$$Ph_{\hat{f}} \leq Ph_{g_{\hat{f}}} + \frac{2}{n} < r(u) + \frac{2}{n}.$$

We have proved that for every  $u \geq 0$ ,

$$\Pr \left( Ph_{\hat{f}} > \frac{2}{n} + \max \left\{ \frac{4}{n}, 4\varepsilon_l^2, \frac{406(d \log(3n) + u)}{n} \right\} \right) \leq e^{-u}.$$

Since

$$\max \left\{ \frac{4}{n}, 4\varepsilon_l^2, \frac{406(d \log(3n) + u)}{n} \right\} \leq 4\varepsilon_l^2 + \frac{406 d \log(3n)}{n} + \frac{406u}{n},$$

we get

$$\Pr \left( Ph_{\hat{f}} > 4\varepsilon_l^2 + \frac{406 d \log(3n) + 2}{n} + \frac{406u}{n} \right) \leq e^{-u}.$$

Integrating this tail bound,

$$\mathbb{E}[Ph_{\hat{f}}] \leq 4\varepsilon_l^2 + \frac{406 d \log(3n) + 2}{n} + \frac{406}{n} \int_0^\infty e^{-u} du,$$

hence

$$\mathbb{E}[h_{\hat{f}}] = \mathbb{E}[Ph_{\hat{f}}] \leq 4\varepsilon_l^2 + \frac{406 d \log(3n) + 408}{n}.$$

This is the desired fast-rate bound.  $\square$

## C.6 Proof of Main Result (Proposition 1)

*Proof.* Since both  $\hat{\eta}_1$  and  $\hat{\eta}_2$  are ERM in the same class  $\mathcal{P}_l$  with  $\{0, 1\}$ -valued responses, we give the argument once for a generic calibration function  $\eta$  estimated by  $\hat{f} = \arg \min_{f \in \mathcal{P}_l} (1/n) \sum (Z_i - f(S_i))^2$ , where  $Z_i \in \{0, 1\}$ .

**Step 1: Approximation error.** By Corollary 1, there exists  $f^* \in \mathcal{P}_l$  (the clipped best polynomial approximation to  $\eta$ ) with  $\|f^* - \eta\|_\infty \leq \varepsilon_l = O(\theta^{-m}) = O(n^{-2})$  by our choice of  $m$ .

**Step 2: Excess risk via the Bernstein condition.** Define the excess loss  $h_f(S, Z) = (f(S) - Z)^2 - (f^*(S) - Z)^2$ . We verify three properties:

(a) *Excess risk equals excess  $L^2$  error:*  $\mathbb{E}[h_f] = \|f - \eta\|_{L^2(P)}^2 - \|f^* - \eta\|_{L^2(P)}^2$ .

This follows by expanding:  $h_f = (f - f^*)(f + f^* - 2Z)$ , so  $\mathbb{E}[h_f | S] = (f - f^*)(f + f^* - 2\eta) = (f - \eta)^2 - (f^* - \eta)^2$ .

(b) *Boundedness:*  $|h_f| \leq |f - f^*| \cdot |f + f^* - 2Z| \leq 1 \cdot 4 = 4$ , since  $f, f^* \in [0, 1]$  and  $Z \in \{0, 1\}$ .

(c) *Bernstein condition:*  $\mathbb{E}[h_f^2] \leq 16\|f - f^*\|_{L^2(P)}^2$ , since  $h_f^2 \leq 16(f - f^*)^2$ . Furthermore,

$$\begin{aligned} \|f - f^*\|_{L^2}^2 &= \|(f - \eta) - (f^* - \eta)\|_{L^2}^2 \\ &\leq 2\|f - \eta\|_{L^2}^2 + 2\|f^* - \eta\|_{L^2}^2 \\ &= 2\mathbb{E}[h_f] + 2\|f^* - \eta\|_{L^2}^2 + 2\|f^* - \eta\|_{L^2}^2 \\ &\leq 2\mathbb{E}[h_f] + 4\varepsilon_l^2. \end{aligned}$$

$$\text{So } \mathbb{E}[h_f^2] \leq 32\mathbb{E}[h_f] + 64\varepsilon_l^2.$$

**Step 3: Fast rate with explicit constants.** Since, by Step 2(a),

$$\mathbb{E}[h_{\hat{f}}] = \|\hat{f} - \eta\|_{L^2(P)}^2 - \|f^* - \eta\|_{L^2(P)}^2,$$

and  $\|f^* - \eta\|_{L^2(P)} \leq \varepsilon_l$ , it follows from lemma 5 that

$$\mathbb{E}\|\hat{f} - \eta\|_{L^2(P)}^2 \leq 5\varepsilon_l^2 + \frac{406 d \log(3n) + 408}{n}.$$

**Step 4: From  $L^2$  error to  $CE_2$ .** Apply the bound from Step 3 separately to the two calibration functions  $\eta_1, \eta_2$ . For  $j \in \{1, 2\}$ , let

$$A_n := 5\varepsilon_l^2 + \frac{406 d \log(3n) + 408}{n},$$

so that

$$\mathbb{E}[\|\hat{\eta}_j - \eta_j\|_{L^2(P)}^2] \leq A_n.$$

By Cauchy–Schwarz and then Jensen’s inequality,

$$\mathbb{E}[\|\hat{\eta}_j - \eta_j\|_{L^1(P)}] \leq \mathbb{E}[\|\hat{\eta}_j - \eta_j\|_{L^2(P)}] \leq \left(\mathbb{E}[\|\hat{\eta}_j - \eta_j\|_{L^2(P)}^2]\right)^{1/2} \leq \sqrt{A_n}.$$

Now write

$$\tilde{v} := \tilde{m}^2 + \tilde{\sigma}_f^2.$$

The perturbed second-order calibration error is

$$CE_2^{\text{pert}} = \mathbb{E}[\eta_1(\tilde{S}) - \tilde{m}] + \mathbb{E}[\eta_2(\tilde{S}) - \tilde{v}].$$

Define the plug-in population analogue

$$CE_2^{\text{plug}} := \mathbb{E}[|\hat{\eta}_1(\tilde{S}) - \tilde{m}|] + \mathbb{E}[|\hat{\eta}_2(\tilde{S}) - \tilde{v}|].$$

Using the reverse triangle inequality,

$$||a - q| - |b - q|| \leq |a - b|,$$

we obtain

$$|CE_2^{\text{plug}} - CE_2^{\text{pert}}| \leq \|\hat{\eta}_1 - \eta_1\|_{L^1(P)} + \|\hat{\eta}_2 - \eta_2\|_{L^1(P)}.$$

Taking expectations and using the previous bound gives

$$\mathbb{E}[|CE_2^{\text{plug}} - CE_2^{\text{pert}}|] \leq 2\sqrt{A_n}.$$

That is,

$$\mathbb{E}[|CE_2^{\text{plug}} - CE_2^{\text{pert}}|] \leq 2 \left(5\varepsilon_l^2 + \frac{406 d \log(3n) + 408}{n}\right)^{1/2}.$$

Finally, with

$$m = \left\lceil \frac{2 \log n}{\log \theta} \right\rceil, \quad d = (l + 1)^2,$$

and  $\varepsilon_l \leq B_\theta \theta^{-l}$  from Corollary 1, we have

$$\varepsilon_l^2 \leq B_\theta^2 \theta^{-2l} \leq B_\theta^2 n^{-4},$$

and therefore

$$\mathbb{E}[|CE_2^{\text{plug}} - CE_2^{\text{pert}}|] \leq 2 \left(5B_\theta^2 n^{-4} + \frac{406 (l + 1)^2 \log(3n) + 408}{n}\right)^{1/2}.$$

In particular,

$$\mathbb{E}[|CE_2^{\text{plug}} - CE_2^{\text{pert}}|] \leq 2 \left(5B_\theta^2 n^{-4} + \frac{406 \left(\frac{2 \log n}{\log \theta} + 2\right)^2 \log(3n) + 408}{n}\right)^{1/2}.$$

This proves the claimed near- $n^{-1/2}$  rate (up to logarithmic factors) for the (expected) quantity  $CE_2^{\text{plug}}$ .

**Step 5: From population to empirical CE.** The preceding steps bound  $\mathbb{E}[\lvert \text{CE}_2^{\text{plug}} - \text{CE}_2^{\text{pert}} \rvert]$ , where  $\text{CE}_2^{\text{plug}} = \mathbb{E}[\lvert \hat{\eta}_1(\tilde{S}) - \tilde{m} \rvert] + \mathbb{E}[\lvert \hat{\eta}_2(\tilde{S}) - \tilde{v} \rvert]$  is evaluated under the *population* measure. The estimator (7) uses the *empirical* measure over the same sample, so we must control the difference.

For any fixed  $f \in \mathcal{P}_l$  the map  $s \mapsto \lvert f(s) - \tilde{m} \rvert$  takes values in  $[0, 1]$ . Define the function class

$$\mathcal{G}_l = \{ (s, \tilde{m}, \tilde{v}) \mapsto \lvert f(s) - \tilde{m} \rvert + \lvert g(s) - \tilde{v} \rvert : f, g \in \mathcal{P}_l \}.$$

Every member of  $\mathcal{G}_l$  is bounded in  $[0, 2]$ . We now bound its covering number.

For any fixed constant  $c$ , the map  $t \mapsto \lvert t - c \rvert$  is 1-Lipschitz, so for any  $f_1, f_2 \in \mathcal{P}_l$  and any  $c$ ,

$$\sup_s \lvert \lvert f_1(s) - c \rvert - \lvert f_2(s) - c \rvert \rvert \leq \sup_s \lvert f_1(s) - f_2(s) \rvert = \|f_1 - f_2\|_\infty.$$

Therefore, if  $\{f^{(1)}, \dots, f^{(N_1)}\}$  is an  $\epsilon$ -cover of  $\mathcal{P}_l$  in  $\|\cdot\|_\infty$ , then for every  $f \in \mathcal{P}_l$  there exists  $f^{(k)}$  with  $\sup_s \lvert \lvert f(s) - c \rvert - \lvert f^{(k)}(s) - c \rvert \rvert \leq \epsilon$ .

Now consider a pair  $(f, g) \in \mathcal{P}_l \times \mathcal{P}_l$  and choose respective  $\epsilon$ -approximants  $f^{(k)}, g^{(j)}$ . By the triangle inequality applied to the sum defining  $\mathcal{G}_l$ ,

$$\lVert (\lvert f(\cdot) - \tilde{m} \rvert + \lvert g(\cdot) - \tilde{v} \rvert) - (\lvert f^{(k)}(\cdot) - \tilde{m} \rvert + \lvert g^{(j)}(\cdot) - \tilde{v} \rvert) \rVert_\infty \leq \|f - f^{(k)}\|_\infty + \|g - g^{(j)}\|_\infty \leq 2\epsilon.$$

Hence an  $\epsilon$ -cover of  $\mathcal{P}_l$  of size  $N_1$  induces a  $2\epsilon$ -cover of  $\mathcal{G}_l$  of size  $N_1^2$ . Substituting  $\epsilon/2$  and applying lemma 4:

$$\log N(\epsilon, \mathcal{G}_l, \|\cdot\|_\infty) \leq 2 \log N\left(\frac{\epsilon}{2}, \mathcal{P}_l, \|\cdot\|_\infty\right) \leq 2(l+1)^2 \log \frac{6}{\epsilon} = 2d \log \frac{6}{\epsilon}.$$

We now bound

$$U := \sup_{h \in \mathcal{G}_l} \left| \frac{1}{n} \sum_{i=1}^n h(Z_i) - \mathbb{E}[h(Z)] \right|,$$

where  $Z_i = (S_i, \tilde{m}_i, \tilde{v}_i)$  are i.i.d.

*Discretisation.* Fix  $\epsilon = 1/n$  and let  $\mathcal{N} \subset \mathcal{G}_l$  be an  $(1/n)$ -cover of  $\mathcal{G}_l$  in  $\|\cdot\|_\infty$ . By the covering-number bound derived above,

$$|\mathcal{N}| \leq N\left(\frac{1}{n}, \mathcal{G}_l, \|\cdot\|_\infty\right) \leq (6n)^{2(l+1)^2}.$$

*Concentration on the cover.* For any fixed  $h \in \mathcal{N}$ , the random variables  $h(Z_1), \dots, h(Z_n)$  are i.i.d. in  $[0, 2]$ . By Hoeffding's inequality (with range  $2 - 0 = 2$ ), for every  $t > 0$ :

$$\Pr\left(\left|\frac{1}{n} \sum_{i=1}^n h(Z_i) - \mathbb{E}[h(Z)]\right| > t\right) \leq 2 \exp\left(-\frac{nt^2}{2}\right).$$

A union bound over  $\mathcal{N}$  gives

$$\Pr\left(\max_{h \in \mathcal{N}} \left|\frac{1}{n} \sum_{i=1}^n h(Z_i) - \mathbb{E}[h(Z)]\right| > t\right) \leq 2|\mathcal{N}| \exp\left(-\frac{nt^2}{2}\right) \leq 2(6n)^{2(l+1)^2} \exp\left(-\frac{nt^2}{2}\right). \quad (15)$$

*Extension to all of  $\mathcal{G}_l$ .* For any  $h \in \mathcal{G}_l$ , choose  $h' \in \mathcal{N}$  with  $\|h - h'\|_\infty \leq 1/n$ . Then

$$\left|\frac{1}{n} \sum_i h(Z_i) - \mathbb{E}[h(Z)]\right| \leq \left|\frac{1}{n} \sum_i h'(Z_i) - \mathbb{E}[h'(Z)]\right| + 2\|h - h'\|_\infty \leq \left|\frac{1}{n} \sum_i h'(Z_i) - \mathbb{E}[h'(Z)]\right| + \frac{2}{n},$$

where the first inequality is the triangle inequality applied to both the empirical and population terms. Taking the supremum over  $h$ , and combining with (15), we obtain a tail bound for  $U := \sup_{h \in \mathcal{G}_l} \left|\frac{1}{n} \sum_{i=1}^n h(Z_i) - \mathbb{E}[h(Z)]\right|$ :

$$\Pr\left(U > t + \frac{2}{n}\right) \leq 2(6n)^{2(l+1)^2} \exp\left(-\frac{nt^2}{2}\right), \quad t > 0. \quad (16)$$

*Expectation bound.* Using  $\mathbb{E}[U] = \int_0^\infty \Pr(U > s) ds$  and the substitution  $s = t + 2/n$ ,

$$\mathbb{E}[U] \leq \frac{2}{n} + \int_0^\infty \min\left(1, 2(6n)^{2(l+1)^2} e^{-nt^2/2}\right) dt.$$

Define

$$t^* = \sqrt{\frac{4(l+1)^2 \log(6n) + 2 \log 2}{n}},$$

chosen so that  $2(6n)^{2(l+1)^2} \exp(-n(t^*)^2/2) = 1$ . Splitting the integral at  $t^*$ :

$$\int_0^\infty \min(\dots) dt \leq t^* + \int_{t^*}^\infty 2(6n)^{2(l+1)^2} e^{-nt^2/2} dt.$$

For the tail integral, note that for  $t \geq t^* > 0$  we have  $1 \leq t/t^*$ , so

$$\int_{t^*}^\infty e^{-nt^2/2} dt \leq \frac{1}{t^*} \int_{t^*}^\infty t e^{-nt^2/2} dt = \frac{1}{t^*} \left[ -\frac{1}{n} e^{-nt^2/2} \right]_{t^*}^\infty = \frac{e^{-n(t^*)^2/2}}{nt^*}.$$

Multiplying by the prefactor and using the definition of  $t^*$ :

$$2(6n)^{2(l+1)^2} \cdot \frac{e^{-n(t^*)^2/2}}{nt^*} = \frac{1}{nt^*}.$$

Therefore

$$\mathbb{E}[U] \leq \frac{2}{n} + t^* + \frac{1}{nt^*} = \frac{2}{n} + \sqrt{\frac{4(l+1)^2 \log(6n) + 2 \log 2}{n}} + \frac{1}{\sqrt{n(4(l+1)^2 \log(6n) + 2 \log 2)}}. \quad (17)$$

*Application to  $\widehat{\text{CE}}_2$ .* Since  $(\hat{\eta}_1, \hat{\eta}_2) \in \mathcal{P}_l \times \mathcal{P}_l$  regardless of the data realisation (the ERM always returns an element of the hypothesis class), the random function  $z \mapsto |\hat{\eta}_1(z) - \tilde{m}| + |\hat{\eta}_2(z) - \tilde{v}|$  lies in  $\mathcal{G}_l$ , and the supremum  $U$  controls this particular instance. Concretely,  $|\widehat{\text{CE}}_2 - \text{CE}_2^{\text{plug}}| \leq U$ , so (17) gives

$$\mathbb{E}[|\widehat{\text{CE}}_2 - \text{CE}_2^{\text{plug}}|] \leq \frac{2}{n} + \sqrt{\frac{4(l+1)^2 \log(6n) + 2 \log 2}{n}} + \frac{1}{\sqrt{n(4(l+1)^2 \log(6n) + 2 \log 2)}}.$$

*Combining with Step 4.* By the triangle inequality,

$$\mathbb{E}[|\widehat{\text{CE}}_2 - \text{CE}_2^{\text{pert}}|] \leq \mathbb{E}[|\widehat{\text{CE}}_2 - \text{CE}_2^{\text{plug}}|] + \mathbb{E}[|\text{CE}_2^{\text{plug}} - \text{CE}_2^{\text{pert}}|].$$

The first term is bounded above. The second term was bounded in Step 4:

$$\mathbb{E}[|\text{CE}_2^{\text{plug}} - \text{CE}_2^{\text{pert}}|] \leq 2 \left( 5B_\theta^2 n^{-4} + \frac{406(l+1)^2 \log(3n) + 408}{n} \right)^{1/2}.$$

With  $l = \lceil 2 \log n / \log \theta \rceil$ , both terms are  $O(\log^{3/2} n / \sqrt{n})$ : the dominant contribution in each is the  $\sqrt{(l+1)^2 \log n / n}$  factor, and  $(l+1)^2 = O(\log^2 n)$ . This proves the rate claimed in equation (8).  $\square$

## D Moments vs Wasserstein Distance for Defining Calibration

In this appendix we relate our definition of second-order calibration (Definition 1) to the  $k^{\text{th}}$ -order calibration framework of Ahdriz et al. [2025]. Note that our treatment is more general than that by Ahdriz et al. [2025] in that we don't rely on any partition of the input space.<sup>3</sup> However, we are also less general in that we only consider a specialization to binary labels  $Y = \{0, 1\}$  and snapshot size  $k = 2$ .

<sup>3</sup>In order to derive the equivalence between our definition and that of Ahdriz et al. [2025], we use a fixed partition  $[\cdot]$  (because their framework requires it).

## D.1 Preliminaries: symmetrized snapshots

A 2-snapshot for an instance  $x$  is a pair  $(y_1, y_2) \in \{0, 1\}^2$  with  $y_1, y_2 \mid x \stackrel{\text{iid}}{\sim} f^*(x)$ . Following Ahdriz et al. [2025], we identify each snapshot with its *empirical distribution* (normalized histogram):

$$\text{Unif}(y_1, y_2)(y) := \frac{1}{2} \sum_{i=1}^2 \mathbf{1}[y_i = y], \quad y \in \{0, 1\}. \quad (18)$$

Each element of  $\{0, 1\}^2$  receives equal weight  $1/k = 1/2$  in the histogram; the name Unif refers to this equal weighting, *not* to the resulting distribution being uniform over  $Y$ . Concretely,

$$(0, 0) \mapsto (1, 0), \quad (0, 1), (1, 0) \mapsto \left(\frac{1}{2}, \frac{1}{2}\right), \quad (1, 1) \mapsto (0, 1),$$

where we write distributions as vectors  $(p_0, p_1)$  over  $\{0, 1\}$ . Since the snapshot is i.i.d., the order of the tuple is immaterial, so the symmetrised snapshot space is

$$Y^{(2)} = \left\{0, \frac{1}{2}, 1\right\} \subset \Delta Y,$$

a set of three atoms. Distributions over  $Y^{(2)}$  are parametrised by a probability vector  $(q_0, q_{1/2}, q_1)$ .

## D.2 The two definitions

**Our definition (Definition 1, specialized to a partition).** Fix a partition  $[\cdot]$  of  $\mathcal{X}$ . Define the calibration functions

$$\eta_1(s) = \mathbb{E}[Y \mid S(X) = s], \quad \eta_2(s) = \mathbb{E}[f^*(X)^2 \mid S(X) = s],$$

with  $S(X) = (m(X), \sigma^2(X))$  and  $v = m^2 + \sigma^2$ . The second-order calibration error is

$$\text{CE}_2 = \mathbb{E}[|\eta_1(S) - m|] + \mathbb{E}[|\eta_2(S) - v|]. \quad (19)$$

When the conditioning is taken with respect to the partition (i.e.  $\eta_1([x]) = \mathbb{E}[f^*(X) \mid X \in [x]]$  and  $\eta_2([x]) = \mathbb{E}[f^*(X)^2 \mid X \in [x]]$ ), the pointwise moment errors on a partition element  $[x]$  are

$$\delta_1([x]) = |\eta_1([x]) - m([x])|, \quad \delta_2([x]) = |\eta_2([x]) - v([x])|. \quad (20)$$

**Ahdriz et al.'s definition 2.3.** A 2-snapshot predictor  $g: \mathcal{X} \rightarrow \Delta Y^{(2)}$  is  $\varepsilon$ -second-order calibrated with respect to a partition  $[\cdot]$  if, for all  $x \in \mathcal{X}$ ,

$$W_1(g(x), \text{proj}_2 f^*([x])) \leq \varepsilon, \quad (21)$$

where  $W_1$  denotes the Wasserstein-1 distance on  $\Delta \Delta Y$  with the  $\ell_1$  distance on  $\Delta Y$  as the ground metric, and  $\text{proj}_2 f^*([x])$  is the true distribution of symmetrised 2-snapshots drawn from  $[x]$ .

**Remark 2** (Worst-case vs. average). Ahdriz et al. [2025] require (21) for all equivalence classes  $[x]$  (worst-case). They note in footnote 4 that a natural relaxation requires (21) only with high probability over equivalence classes drawn according to the marginal  $D_X$ . We call this the relaxed variant: for a given  $\delta > 0$ ,

$$\Pr_{[x] \sim D_X} \left[ W_1(g(x), \text{proj}_2 f^*([x])) > \varepsilon \right] \leq \delta. \quad (22)$$

Our quantity  $\text{CE}_2$  is an average (expectation under  $D_X$ ) and therefore corresponds most naturally to this relaxed variant.

## D.3 Relating the two definitions

We now establish the precise relationship. The key is a pointwise sandwich between the Wasserstein error and the moment errors.

**Lemma 6** (Pointwise sandwich). Fix a partition element  $[x]$ . Let  $\delta_1([x]), \delta_2([x])$  be as in (20) and  $W_1([x])$  as in (21). Then

$$\delta_1([x]) + \delta_2([x]) \leq \frac{3}{2} W_1([x]) \leq 3(\delta_1([x]) + \delta_2([x])). \quad (23)$$

*Proof.* A distribution over  $Y^{(2)} = \{0, \frac{1}{2}, 1\}$  is a vector  $(q_0, q_{1/2}, q_1)$ . The predictor's output corresponds to  $(q_0, q_{1/2}, q_1)$  and the true snapshot distribution to  $(p_0, p_{1/2}, p_1)$ , with

$$p_1 = \mu_2, \quad p_{1/2} = 2(\mu_1 - \mu_2), \quad p_0 = 1 - 2\mu_1 + \mu_2,$$

where  $\mu_j = \mathbb{E}_{x \sim [x]}[f^*(x)^j]$ . For the predictor's output, let  $m([x])$  and  $v([x]) = m([x])^2 + \sigma^2([x])$  denote the shared values of  $m$  and  $v$  on the partition element  $[x]$ . The predicted snapshot distribution is

$$q_1 = v([x]), \quad q_{1/2} = 2(m([x]) - v([x])), \quad q_0 = 1 - 2m([x]) + v([x]).$$

Write  $\Delta_j = p_j - q_j$  for  $j \in \{0, \frac{1}{2}, 1\}$ , so that  $\Delta_0 + \Delta_{1/2} + \Delta_1 = 0$ . We now compute  $W_1([x])$ . Each atom of  $Y^{(2)}$  is a distribution over  $\{0, 1\}$ :  $0 \leftrightarrow (1, 0)$ ,  $\frac{1}{2} \leftrightarrow (\frac{1}{2}, \frac{1}{2})$ ,  $1 \leftrightarrow (0, 1)$ . The ground metric is the  $\ell_1$  distance inherited from  $\Delta Y$ :

$$d(0, \frac{1}{2}) = 1, \quad d(\frac{1}{2}, 1) = 1, \quad d(0, 1) = 2.$$

Since  $d(0, 1) = d(0, \frac{1}{2}) + d(\frac{1}{2}, 1)$ , it is never cheaper to transport mass directly between the outer atoms than to route it through  $\frac{1}{2}$ . The optimal plan is therefore determined by two edge flows: let  $\phi_1$  be the net signed flow from atom 0 to atom  $\frac{1}{2}$ , and  $\phi_2$  from atom  $\frac{1}{2}$  to atom 1. Mass balance at each atom gives  $\phi_1 = \Delta_0$  and  $\phi_2 = \Delta_0 + \Delta_{1/2} = -\Delta_1$ , so

$$W_1([x]) = |\phi_1| \cdot d(0, \frac{1}{2}) + |\phi_2| \cdot d(\frac{1}{2}, 1) = |\Delta_0| + |\Delta_1|.$$

Meanwhile, the moment errors are

$$\delta_1([x]) = |\mu_1 - m| = \frac{1}{2}|\Delta_{1/2} + 2\Delta_1| = \frac{1}{2}|\Delta_0 - \Delta_1|, \quad \delta_2([x]) = |\mu_2 - v| = |\Delta_1|.$$

*Upper bound.* By the triangle inequality,  $|\Delta_0| \leq |\Delta_0 - \Delta_1| + |\Delta_1| = 2\delta_1 + \delta_2$ , so

$$W_1 = |\Delta_0| + |\Delta_1| \leq 2\delta_1 + 2\delta_2.$$

This is the same as

$$\frac{3}{2}W_1 \leq 3\delta_1 + 3\delta_2$$

*Lower bound.* We have  $\delta_2 = |\Delta_1| \leq W_1$  and  $\delta_1 = \frac{1}{2}|\Delta_0 - \Delta_1| \leq \frac{1}{2}(|\Delta_0| + |\Delta_1|) = \frac{1}{2}W_1$ , so  $\delta_1 + \delta_2 \leq \frac{3}{2}W_1$ .  $\square$

We can now state the three main properties.

**Property 1** (Equivalence at zero error).  $\text{CE}_2 = 0$  if and only if, for  $D_X$ -almost every equivalence class  $[x]$ ,  $W_1([x]) = 0$ .

*Proof.* By (23),  $W_1([x]) = 0$  iff  $\delta_1([x]) + \delta_2([x]) = 0$ . Since  $\text{CE}_2 = \mathbb{E}_{[x]}[\delta_1([x]) + \delta_2([x])]$ , the expectation vanishes iff the integrand vanishes  $D_X$ -a.e.  $\square$

**Property 2** (Ahdritz approximate calibration implies bounded  $\text{CE}_2$ ). If  $g$  is  $\varepsilon$ -second-order calibrated in the sense of (21) (worst-case), then

$$\text{CE}_2 \leq \frac{3}{2}\varepsilon.$$

*Proof.* For every  $[x]$ , the lower bound in (23) gives  $\delta_1([x]) + \delta_2([x]) \leq \frac{3}{2}\varepsilon$ . Averaging over  $D_X$  yields the claim.  $\square$

**Property 3** (Bounded  $\text{CE}_2$  implies relaxed Ahdritz calibration). If  $\text{CE}_2 \leq \varepsilon$ , then for every  $\delta > 0$ ,

$$\Pr_{[x] \sim D_X} [W_1([x]) > 2\varepsilon/\delta] \leq \delta.$$

In particular,  $g$  satisfies the relaxed variant (22) with parameters  $(\varepsilon', \delta)$  for  $\varepsilon' = 2\varepsilon/\delta$ .

However,  $\text{CE}_2 \leq \varepsilon$  does not in general imply a uniform (worst-case) bound on  $W_1([x])$  over all partition elements, since  $\text{CE}_2$  is an average quantity.

*Proof.* The upper bound in (23) gives  $W_1([x]) \leq 2(\delta_1([x]) + \delta_2([x]))$ , so

$$\mathbb{E}_{[x]}[W_1([x])] \leq 2\text{CE}_2 \leq 2\varepsilon.$$

Markov's inequality yields the stated tail bound.  $\square$

**Remark 3.** *If one adopts the relaxed (high-probability) variant of Ahdriz et al.'s definition, then Properties 2 and 3 together show that the two notions are quantitatively comparable: writing  $\overline{W}_1 = \mathbb{E}_{[x]}[W_1([x])]$  for the average Wasserstein error,*

$$\frac{1}{2} \overline{W}_1 \leq \text{CE}_2 \leq \frac{3}{2} \overline{W}_1.$$

## E Matching Lower Bound on Rate

In this section, we prove Proposition 2.

*Proof.*

### E.1 The two-point family

Take  $\mathcal{X}$  a singleton (suppress  $X$ ) and use the boundary constant predictor

$$S(x) \equiv (m_0, \sigma_0^2) := (1, 0).$$

Since  $m_0 = 1$  forces  $m_0(1 - m_0) = 0$ , the only valid value is  $\sigma_0^2 = 0$ ; the score is therefore the deterministic point  $(1, 0)$ , which lies in the feasible region. The sech perturbation produces  $\tilde{S} = (\tilde{m}, \tilde{\sigma}^2)$ , where  $\tilde{m}$  has density  $k_h(\cdot | 1)$  on  $[0, 1]$  and  $\tilde{\sigma}^2$  has density  $k_h(\cdot | 0)$  on  $[0, 1/4]$ , independently. The law of  $\tilde{S}$  is the *same* under both  $P_0$  and  $P_1$ .

For  $b \in \{0, 1\}$ , let  $P_b$  be the law in which  $f^* \equiv p_b$ , with

$$p_0 := \frac{1}{16}, \quad p_1 := \frac{1}{16} + \varepsilon,$$

for an  $\varepsilon \in (0, 1/16]$  to be chosen later. So  $Y_i^{(j)} \stackrel{\text{iid}}{\sim} \text{Bernoulli}(p_b)$ , independent of  $\tilde{S}$ .

### E.2 The calibration error has a clean closed form

Since  $S$  is constant,  $\tilde{S}$  is independent of the labels and the calibration functions are themselves constants:

$$\eta_1(\tilde{S}) = p_b, \quad \eta_2(\tilde{S}) = p_b^2.$$

(Both are trivially analytic, satisfying the structural assumptions of the main paper.) Substituting:

$$\text{CE}_2^{\text{pert}}(P_b) = \underbrace{\mathbb{E}[|p_b - \tilde{m}|]}_{=: \phi(p_b)} + \underbrace{\mathbb{E}[|p_b^2 - W|]}_{=: \psi(p_b)}, \quad W := \tilde{m}^2 + \tilde{\sigma}^2. \quad (24)$$

### E.3 Key lemma: stochastic dominance, uniform in $h$

**Lemma 7.** *For  $m_0 = 1$  and every  $h > 0$ ,*

$$F_{\tilde{m}}(p) \leq p \quad \text{for all } p \in [0, 1].$$

*Equivalently,  $\tilde{m}$  stochastically dominates  $U[0, 1]$ .*

*Proof.* Let  $G(x) := \int_0^x \text{sech}(v) dv$ . We have  $G(0) = 0$ ,  $G'(x) = \text{sech}(x) > 0$ , and  $G''(x) = -\text{sech}(x) \tanh(x) \leq 0$  for  $x \geq 0$ , so  $G$  is concave on  $[0, \infty)$ .

Substituting  $v = (1 - t)/h$  in the integral defining  $F_{\tilde{m}}$ :

$$F_{\tilde{m}}(p) = \frac{\int_0^p \text{sech}((t-1)/h) dt}{\int_0^1 \text{sech}((u-1)/h) du} = 1 - \frac{G((1-p)/h)}{G(1/h)}.$$

By concavity of  $G$  on  $[0, \infty)$  and  $G(0) = 0$ , for any  $\theta \in [0, 1]$  and  $x \geq 0$ ,

$$G(\theta x) = G(\theta x + (1 - \theta) \cdot 0) \geq \theta G(x) + (1 - \theta) G(0) = \theta G(x).$$

Setting  $\theta = 1 - p$  and  $x = 1/h$ :  $G((1-p)/h) \geq (1-p)G(1/h)$ , so  $F_{\tilde{m}}(p) \leq 1 - (1-p) = p$ .  $\square$

#### E.4 The gap

We bound  $\phi$  and  $\psi$  separately by integrating their derivatives.

**First moment.** The function  $\phi(p) = \mathbb{E}|p - \tilde{m}|$  is convex and differentiable everywhere on  $(0, 1)$  (since  $\tilde{m}$  has a continuous density), with

$$\phi'(p) = 2F_{\tilde{m}}(p) - 1 \leq 2p - 1$$

by Lemma 7. Integrating from  $p_0$  to  $p_1 = p_0 + \varepsilon$ ,

$$\begin{aligned} \phi(p_1) - \phi(p_0) &\leq \int_{p_0}^{p_1} (2p - 1) dp = (p_1^2 - p_0^2) - (p_1 - p_0) \\ &= \varepsilon(p_0 + p_1 - 1) \leq \varepsilon\left(\frac{1}{16} + \frac{1}{8} - 1\right) = -\frac{13}{16}\varepsilon, \end{aligned}$$

using  $p_1 \leq 1/8$ .

**Second moment.** Differentiation under the expectation (justified by the Lipschitz continuity in  $p$  of  $|p^2 - W|$  and the continuous density of  $W$ ) gives

$$\psi'(p) = 2p(2F_W(p^2) - 1), \quad |\psi'(p)| \leq 2p.$$

Hence

$$|\psi(p_1) - \psi(p_0)| \leq \int_{p_0}^{p_1} 2p dp = p_1^2 - p_0^2 \leq 2p_1 \varepsilon \leq \frac{\varepsilon}{4}.$$

**Combining.** From (24),

$$\text{CE}_2^{\text{pert}}(P_0) - \text{CE}_2^{\text{pert}}(P_1) = (\phi(p_0) - \phi(p_1)) + (\psi(p_0) - \psi(p_1)) \geq \frac{13}{16}\varepsilon - \frac{1}{4}\varepsilon = \frac{9}{16}\varepsilon \geq \frac{\varepsilon}{2}. \quad (25)$$

#### E.5 KL bound

The perturbed scores carry no information about  $b$  (their law is identical under  $P_0, P_1$  and they are independent of the labels), so each observation under  $P_b$  is informationally equivalent to two i.i.d. Bernoulli( $p_b$ ) draws. With both  $p_0 = 1/16$  and  $p_1 \leq 1/8$ ,  $p_1(1 - p_1) \geq (1/16)(15/16) \geq 1/18$ , so

$$\text{KL}(\text{Bernoulli}(p_0) \parallel \text{Bernoulli}(p_1)) \leq \frac{(p_1 - p_0)^2}{p_1(1 - p_1)} \leq 18\varepsilon^2.$$

Tensorizing,

$$\text{KL}(P_0^{\otimes n} \parallel P_1^{\otimes n}) \leq 36n\varepsilon^2. \quad (26)$$

#### E.6 Le Cam

Le Cam's two-point lemma [Polyanskiy and Wu, 2025, Chapter 31]: for any real-valued estimator  $\hat{\theta}$ ,

$$\max_{b \in \{0,1\}} \mathbb{E}_{P_b^{\otimes n}}[|\hat{\theta} - \theta(P_b)|] \geq \frac{1}{2} |\theta(P_1) - \theta(P_0)| \cdot (1 - \text{TV}(P_0^{\otimes n}, P_1^{\otimes n})).$$

By Pinsker and (26),  $\text{TV} \leq \sqrt{\text{KL}/2} \leq \sqrt{18n\varepsilon^2} = 3\varepsilon\sqrt{2n}$ .

**Choosing  $\varepsilon$ .** Set

$$\varepsilon := \frac{1}{6\sqrt{2n}}.$$

Then  $\text{TV} \leq 1/2$ , hence  $1 - \text{TV} \geq 1/2$ . For  $n \geq 4$  we also have  $\varepsilon \leq 1/16$ , so the gap bound (25) applies. Combining (25) with Le Cam:

$$\max_{b \in \{0,1\}} \mathbb{E}_{P_b^{\otimes n}}[|\widehat{\text{CE}}_2 - \text{CE}_2^{\text{pert}}(P_b)|] \geq \frac{1}{2} \cdot \frac{\varepsilon}{2} \cdot \frac{1}{2} = \frac{\varepsilon}{8} = \frac{1}{48\sqrt{2n}}.$$

For  $n \in \{1, 2, 3\}$  the bound holds trivially with a smaller constant. Setting  $c := 1/(48\sqrt{2})$  — an absolute constant, independent of  $h$  — proves Proposition 2.  $\square$

## **F Compute Resources**

The expected compute requirements are modest: all experiments can be run on a standard laptop.

## **G Open Questions**

We think the following questions would be useful avenues for further work.

1. Extension to multiclass classification (we handle the binary case).
2. Look at removing logarithmic factors from the upper bound (we match lower an upper bounds up to logarithmic factors).
3. Look at alternatives to perturbation (while the work Gupta et al. [2020] implies structural assumptions are needed, maybe there exists a less ‘invasive’ form of meeting them than the perturbation).